

Short-time Fokker-Planck propagator beyond the Gaussian approximation

Julian Kappler*

*Arnold Sommerfeld Center for Theoretical Physics (ASC), Department of Physics,
Ludwig-Maximilians-Universität München, Theresienstraße 37, D-80333 Munich, Germany*

(Dated: May 29, 2024)

We present a perturbation approach to calculate the short-time propagator, or transition density, of the one-dimensional Fokker-Planck equation, to in principle arbitrary order in the time increment. Our approach preserves probability exactly and allows us to evaluate expectation values of analytical observables to in principle arbitrary accuracy; to showcase this, we derive perturbation expansions for the moments of the spatial increment, the finite-time Kramers-Moyal coefficients, and the mean medium entropy production rate. For an explicit multiplicative-noise system with available analytical solution, we validate all our perturbative results. Throughout, we compare our perturbative results to those obtained from the widely used Gaussian approximation of the short-time propagator; we demonstrate that this Gaussian propagator leads to errors that can be many orders of magnitude larger than those resulting from our perturbation approach. Potential applications of our results include parametrizing diffusive stochastic dynamics from observed time series, and sampling path spaces of stochastic trajectories numerically.

I. INTRODUCTION

Diffusive stochastic processes are ubiquitous in several branches of science, including physics, chemistry, and biology [1–4]. The time evolution of a reaction coordinate subject to diffusive stochastic dynamics can be described by a stochastic differential equation (SDE), which in the physics literature is usually called the overdamped Langevin equation, or, equivalently, or by its associated Fokker-Planck equation (FPE) [1, 3]. While the former constitutes a description on the level of stochastic realizations of the reaction coordinate, the latter describes the time evolution of the probability density for observing a the reaction coordinate at a given location. Of particular interest here is the short-time propagator, i.e. the distribution of the spatial increment Δx after a short time increment Δt , for a particle starting at a given initial position x_0 . This propagator allows to calculate expectation values, which in turn can be used to parametrize the FPE from observed time series [5–7]. Furthermore, the short-time propagator is a starting point to derive the path-integral representation of the stochastic process via time-slicing [8–19]. In its discretized form, the path integral can be used for Bayesian parameter inference [20–28] or sampling of transition ensembles [29, 30] via Markov Chain Monte Carlo (MCMC); in its continuum form, it has been used to to analyze transitions between metastable states [11, 31, 32] or to quantify irreversibility [13, 33–35].

The most widely used approximate expression for the short-time propagator uses a Gaussian distribution for the spatial increment Δx , and is based on an Euler-Maruyama discretization of the underlying SDE [10–15, 17–19, 36]. There seem to exist few explicitly known approximate short-time propagators beyond the Gaus-

sian approximation in the literature. Elerian [22] provides a closed-form expressions for a short-time propagator based on the Milstein discretization scheme, which has been used in Refs. [23, 28]. Drozdov [37–40] discusses several approximation schemes for the logarithm of the short-time propagator, which are based on the cumulant generation function [39, 40], or a direct power-series ansatz (in powers of the short time increment Δt) in the exponent of the short-time propagator [37, 38]. Using an expansion in Hermite polynomials, Ait-Sahalia [41, 42] also derives an approximation scheme for the logarithm of the short-time propagator. One derivation of his approximation scheme involves a nonlinear coordinate transformation [41, 42], the other [42] uses an expansion both the spatial increment Δx and the time increment Δt of the diffusion process. At the time of submission of the present paper, we became aware of the recent work of Sorokin, Ariel, and Markovich, who derived another approximation scheme for the short-time propagator [43]; their scheme employs stochastic Taylor expansions [44] and, like Ait-Sahalia [42], they express their result in terms of Hermite polynomials. The derivations of Drozdov and Ait-Sahalia both lead to an approximate propagator that ensures the non-negativity of the probability density exactly, but in general does not lead to a properly normalized probability density [42]. Furthermore, since the approximate propagators are generally in the form of an exponential of a function (with the exception of Ref. [43]), it is not straightforward to analytically evaluate expectation value integrals with them.

For one-dimensional reaction coordinates, we here present a perturbation theory approach to calculate the short-time propagator to in principle arbitrary accuracy. The basic underlying ideas are similar to Refs. [41, 42], but our execution differs in several aspects. First, we employ neither a nonlinear coordinate transformation, nor do we simultaneously expand in two variables. Rather, our derivation uses a single linear coordinate transformation, which explicitly encodes the relative scale of the

* jkappler@posteo.de

typical position increment Δx during a short time increment Δt ; this results in a theory with a single perturbation parameter, which is proportional to $\sqrt{\Delta t}$ (as opposed to Ref. [37, 38], where a perturbation series in Δt is used). Second, our approach directly leads to an approximate propagator that is properly normalized at all orders of perturbation theory, but can take negative values in regimes where the perturbation theory ceases to be valid. The non-Gaussian propagators in Ref. [37–42], on the other hand, preserve positivity exactly, but in general are not properly normalized. One advantage of the normalization-preserving propagator (NPP) over the positivity-preserving propagator (PPP) is that the former straightforwardly allows for perturbative evaluation of expectation values. We demonstrate this by deriving explicit perturbative formulas for the moments $\langle \Delta x^n \rangle$, the finite-time Kramers-Moyal coefficients, and the medium entropy production rate.

We supply an accompanying python module called PySTFP [45], where STFP stands for short-time Fokker-Planck. The module contains readily useable symbolic [46] expressions for the NPP with a spatial integrated pointwise error that scales as $\Delta t^{9/2}$. Our module furthermore includes symbolic expressions for the moments $\langle \Delta x^n \rangle$ for $n = 0, 1, 2, 3, 4$ up to an error of the order Δt^5 , the medium entropy production rate and the Gibbs entropy up to an error of the order Δt^5 , and the total entropy production rate up to an error of the order Δt^4 . Additionally, we provide code to reproduce all figures of this paper, and to symbolically evaluate all the power series we consider here (i.e. short-time propagator, moments, Gibbs entropy, medium entropy production rate, total entropy production rate) to in principle arbitrary desired order.

The remainder of this paper is organized as follows. In Sect. II we first introduce the SDE and FPE that describe one-dimensional diffusive stochastic dynamics. We then recall a standard derivation of the Gaussian propagator in Sect. III. In the subsequent Sect. IV, we derive our perturbation scheme, and formulate the result both in a normalization-preserving and positivity-preserving representation. In Sect. V we use the normalization-preserving representation of the propagator to derive perturbative expressions for the moments of the position increment, for the first two finite-time Kramers-Moyal coefficients, and for the medium entropy production rate. In Sect. VI, we illustrate all our results with a numerical example, and in Sect. VII we conclude by summarizing our results and discussing their further implications.

The appendices contain more details for our derivations, as well as additional analyses. In particular, in App. B we give the propagator, to second order in the perturbation theory, in both normalization- and positivity-preserving representations, as well as in a midpoint-evaluation scheme. For the latter we discuss the ratio of forward-backward path probabilities, as related to pathwise entropy production [13, 33–35]. Furthermore, in App. D we derive power series expansions

of the Gibbs entropy, as well as the medium- and the total entropy production rate.

II. DIFFUSIVE STOCHASTIC DYNAMICS

We consider the one-dimensional Fokker-Planck equation (FPE) [1–3]

$$\partial_t P = -\partial_x(aP) + \partial_x^2(DP), \quad (1)$$

where $D \equiv D(x)$ is a diffusivity profile, $a \equiv a(x)$ is a drift profile, and where $P \equiv P(x, t | x_0, t_0)$ is the propagator, or transition (probability) density, to find a particle that starts at (x_0, t_0) at the point (x, t) , where $t > t_0$. We assume both drift and diffusivity are independent of time, and seek to calculate a short-time solution to Eq. (1) subject to the boundary conditions

$$P(x, t | x_0, t_0) \rightarrow 0 \quad |x| \rightarrow \infty, \quad (2)$$

and the normalization condition

$$\int_{-\infty}^{\infty} dx P(x, t | x_0, t_0) = 1. \quad (3)$$

Throughout this paper, we switch between (x, t, x_0, t_0) and $(\Delta x, \Delta t, x_0, t_0)$ as independent variables as is convenient, where $\Delta x \equiv x - x_0$, $\Delta t \equiv t - t_0$. We assume x_0, t_0 as fixed and given and, unless important for the context, suppress explicit dependences on those two parameters in the notation.

The FP Eq. (1) is equivalent to the Itô-Langevin equation [1–3]

$$dX_t = a(X_t) dt + \sqrt{2D(X_t)} dB_t. \quad (4)$$

Here, dX_t is the increment of the diffusive stochastic process X_t during a time increment dt , and dB_t is the increment of the Wiener process. In the Itô-Langevin formulation, the delta-peak initial condition is given as $X_{t_0} = x_0$.

III. GAUSSIAN SHORT-TIME PROPAGATOR

For completeness and future reference, we now recall a standard derivation of the approximate propagator $P(x, t | x_0, t_0)$ for a short time increment $\Delta t \equiv t - t_0$ [10, 12, 14, 18, 19, 35, 47, 48].

From a stochastic Taylor expansion of Eq. (4) it follows that for a short time interval Δt , we have [44]

$$\Delta X(\Delta W) = a(x_0)\Delta t + \sqrt{2D(x_0)\Delta t}\Delta W + \mathcal{O}(\Delta t^\beta), \quad (5)$$

where $\Delta X = X_t - x_0$, and where ΔW is a unit normal random variable with density

$$P(\Delta w) = \frac{1}{\sqrt{2\pi}} e^{-\Delta w^2/2}. \quad (6)$$

By the notation $\Delta X(\Delta W)$ on the left-hand side of Eq. (5) we emphasize that the random variable ΔX is a function of the noise increment ΔW . The error in the short-time discretization Eq. (5) is of order Δt^β , with $\beta = 3/2$ for additive noise and $\beta = 1$ for multiplicative noise [44]; this is the statement that the Euler-Maruyama discretization scheme has strong order of convergence Δt for additive noise, and strong order of convergence $\sqrt{\Delta t}$ for multiplicative noise [44].

The probability density to observe an increment $\Delta x \equiv x - x_0$ follows by a change of measure [2]

$$P(\Delta x) = \int_{-\infty}^{\infty} d\Delta w \delta(\Delta X(\Delta w) - \Delta x) P(\Delta w), \quad (7)$$

where δ is the Dirac-delta distribution and $\Delta X(\Delta w)$ is defined in Eq. (5). To evaluate the integral on the right-hand side of Eq. (7), we solve Eq. (5) for ΔW ,

$$\Delta W(\Delta X) = \frac{\Delta X - a(x_0)\Delta t}{\sqrt{2D(x_0)\Delta t}} + \mathcal{O}(\Delta t^{\beta-1/2}). \quad (8)$$

Note that because solving Eq. (5) for ΔW entails dividing the equation by $\sqrt{\Delta t}$, the term $\mathcal{O}(\Delta t^\beta)$ from Eq. (5) leads to a term of order $\mathcal{O}(\Delta t^{\beta-1/2})$ in Eq. (8). From Eq. (8) we obtain in particular the noise increment $\Delta w = \Delta W(\Delta x)$ which corresponds to Δx . Using the usual chain rule for the Dirac-delta distribution [49],

$$\delta(\Delta X(\Delta w) - \Delta x) = \frac{\delta(\Delta w - \Delta W(\Delta x))}{\left. \frac{d\Delta X}{d\Delta W} \right|_{\Delta W(\Delta x)}}, \quad (9)$$

with $d\Delta X/d\Delta W|_{\Delta W(\Delta x)} = \sqrt{2D(x_0)\Delta t}$, the integral on the right-hand side of Eq. (7) then evaluates to

$$P(\Delta x) = \frac{1}{\sqrt{2D(x_0)\Delta t}} P(\Delta W(\Delta x)) \quad (10)$$

$$= \frac{1}{\sqrt{4\pi D(x_0)\Delta t}} \times \exp \left[-\frac{\Delta t}{4D(x_0)} \left(\frac{\Delta x}{\Delta t} - a(x_0) \right)^2 + \mathcal{O}(\Delta t^{\beta-1/2}) \right], \quad (11)$$

where we assume that $\Delta x = \mathcal{O}(\sqrt{\Delta t})$. This is true both if Δx is a typical realization of the Itô-Langevin Eq. (4) or if Δx is a differentiable path, in which case the stronger statement $\Delta x = \mathcal{O}(\Delta t)$ holds.

We stress that even for additive noise, the exponent in the short-time propagator Eq. (11) is only accurate to including order $\sqrt{\Delta t}$. This is ultimately because in solving Eq. (5) for ΔW , we divide the equation by $\sqrt{\Delta t}$.

In principle the above derivation can be extended to arbitrary order by replacing Eq. (5) with a higher-order stochastic Taylor expansion [44]. This was done for additive noise in Ref. [6], where the above derivation is carried out with the order- $\Delta t^{3/2}$ term included in Eq. (5) [44]. The resulting exponent in the short-time propagator from

Ref. [6] indeed differs from Eq. (11) by a term of order Δt . However, in general it does not seem practical to derive the short-time propagator to higher accuracy via time-discretizations of the Itô-Langevin Eq. (4) directly. The reason for this is that, as is apparent in Ref. [6], higher-order stochastic Taylor expansions of the SDE lead to the appearance of an increasing number of correlated random variables on the right-hand side of Eq. (5). The corresponding change of variables Eq. (7) then quickly becomes infeasible. While the approach in Ref. [43] is based on stochastic Taylor expansions, it does not follow the strategy from this section, but instead uses characteristic functions.

In the next section, we consider a derivation of the short-time propagator that is not based on the Itô-Langevin SDE, but on the equivalent description of the stochastic process via the FP Eq. (1).

IV. PERTURBATIVE SHORT-TIME PROPAGATOR

A. Normalization-preserving propagator

For given x_0, t_0 , we now derive a short-time approximation for the propagator $P(x, t | x_0, t_0)$, valid for $\Delta t \equiv t - t_0$ sufficiently small, and subject to the delta-peak initial condition $P(x, t_0 | x_0, t_0) = \delta(x - x_0)$.

Intuitively, we expect the propagator to behave as follows. For very short time Δt , the stochastic dynamics described by Eq. (1) is dominated by the diffusivity (as opposed to the drift). This is most clearly seen by considering the time-discretized Itô-Langevin Eq. (5). For a short time increment, the random noise term scales as $\sqrt{\Delta t}$, whereas the term that contains the deterministic drift scales as Δt . For short enough time increment, the short-time propagator should thus be well-approximated by the free-diffusion propagator with position-independent diffusivity $D(x_0)$. Based on this intuition, our approach is to perturb around this free-diffusion solution, and to calculate corrections to it in powers of $\sqrt{\Delta t}$.

For this we first rewrite Eq. (1) in dimensionless form. We fix a length scale L , and note that the given initial point x_0 leads to a diffusivity scale $D(x_0)$. This in turn defines an associated time scale $\tau_D(x_0) = L^2/D(x_0)$. The diffusivity $D(x_0)$ furthermore gives rise to a time-dependent length scale, namely the typical distance $R(\Delta t)$ a freely diffusing particle subject to diffusivity $D(x_0)$ travels during a short time increment Δt ,

$$R(\Delta t) \equiv \sqrt{2D(x_0)\Delta t}. \quad (12)$$

Using the time scale τ_D and length scale $R(\Delta t)$, we define a dimensionless time-dependent coordinate system

$$\tilde{t}(\Delta t) \equiv \frac{t - t_0}{\tau_D} \equiv \frac{\Delta t}{\tau_D}, \quad (13)$$

$$\tilde{x}(\Delta x, \Delta t) \equiv \frac{x - x_0}{R(\Delta t)} \equiv \frac{\Delta x}{R(\Delta t)}, \quad (14)$$

where, as before, in our notation we suppress the dependence of τ_D , R on the fixed initial position x_0 .

With respect to the coordinates Eqs. (13), (14), we rewrite the FP Eq. (1) in dimensionless form as

$$\tilde{\epsilon}^2 \partial_{\tilde{t}} \tilde{P} = -\partial_{\tilde{x}} \left[(\tilde{\epsilon} \tilde{a} - \tilde{x}) \tilde{P} \right] + \partial_{\tilde{x}}^2 \left(\tilde{D} \tilde{P} \right), \quad (15)$$

with

$$\tilde{\epsilon}(\tilde{t}) \equiv \frac{R(\Delta t)}{L}, \quad (16)$$

$$\tilde{P}(\tilde{x}, \tilde{t}) \equiv R(\Delta t) P(x, t | x_0, t_0), \quad (17)$$

$$\tilde{a}(\tilde{x}) \equiv \frac{\tau_D}{L} a(x), \quad (18)$$

$$\tilde{D}(\tilde{x}) \equiv \frac{D(x)}{D(x_0)}, \quad (19)$$

where (\tilde{x}, \tilde{t}) are related to $(\Delta x, \Delta t)$ via Eqs. (13), (14).

The boundary conditions Eq. (2) become

$$\tilde{P}(\tilde{x}, \tilde{t}) \rightarrow 0 \quad |\tilde{x}| \rightarrow \infty, \quad (20)$$

and the normalization condition Eq. (3) is given in dimensionless form as

$$\int_{-\infty}^{\infty} d\tilde{x} \tilde{P}(\tilde{x}, \tilde{t}) = 1. \quad (21)$$

By definition of $\tilde{\epsilon}$ it holds that $\tilde{\epsilon} = \sqrt{2\tilde{t}} \sim \sqrt{\Delta t}$, so that an expansion of \tilde{P} in powers of $\tilde{\epsilon}$ is a short-time expansion. Furthermore, in Eq. (14) the (on short times) dominant free-diffusion contribution to the spatial increment has been incorporated explicitly via the denominator $R(\Delta t)$, so that for short time we expect that the probability density is only non-negligible for values $|\tilde{x}| \lesssim 1$. We therefore seek a solution of Eq. (15) in the form of a power-series in $\tilde{\epsilon}$, assuming that $\tilde{x} = \mathcal{O}(\tilde{\epsilon}^0)$.

For this, we introduce a power series ansatz

$$\tilde{P}(\tilde{x}, \tilde{t}) = \tilde{P}^{(0)}(\tilde{x}) \left[1 + \tilde{\epsilon}(\tilde{t}) \tilde{\mathcal{Q}}_1(\tilde{x}) + \tilde{\epsilon}^2(\tilde{t}) \tilde{\mathcal{Q}}_2(\tilde{x}) + \dots \right] \quad (22)$$

$$= \tilde{P}^{(0)}(\tilde{x}) \left[\sum_{n=0}^{\infty} \tilde{\epsilon}^n(\tilde{t}) \tilde{\mathcal{Q}}_n(\tilde{x}) \right], \quad (23)$$

where we identify $\tilde{\mathcal{Q}}_0(\tilde{x}) \equiv 1$ (which will be justified further below) and where

$$\tilde{P}^{(0)}(\tilde{x}) = \frac{1}{\sqrt{2\pi}} \exp\left(-\frac{\tilde{x}^2}{2}\right). \quad (24)$$

From the definition of \tilde{x} , Eq. (14), it is evident that Eq. (24) is the free-diffusion solution of a FPE with spatially constant diffusivity $D(x_0)$ and without any deterministic drift; this is precisely the expected behavior of a solution Eq. (1) at asymptotically short times.

In contrast to our perturbation ansatz Eq. (22), Refs. [37–42] consider a power series ansatz in the exponent of the short-time propagator. Furthermore, in

Ref. [41] a change of coordinates similar to Eq. (14) is used, together with a nonlinear change in coordinates that transforms the multiplicative-noise Eq. (14) into an additive-noise system. Our derivation, however, involves no nonlinear coordinate transformations. Conceptually our approach here is similar to Refs. [50, 51] where, for an absorbing-boundary FPE, after a linear coordinate transformation a systematic perturbation theory around an asymptotic solution was developed.

We seek to determine the functions $\tilde{\mathcal{Q}}_k(\tilde{x})$ such that Eq. (22) solves the dimensionless FP Eq. (15), and fulfills the boundary conditions Eq. (20) at each order in $\tilde{\epsilon}$, which at order $\tilde{\epsilon}^k$ read

$$\tilde{\mathcal{Q}}_k(\tilde{x}) \tilde{P}^{(0)}(\tilde{x}) \rightarrow 0 \quad \text{as } |\tilde{x}| \rightarrow \infty. \quad (25)$$

To derive a hierarchy of equations from Eq. (15), we first Taylor expand $a(x)$, $D(x)$ around x_0 . In dimensionless units this yields

$$\tilde{a}(\tilde{x}, \tilde{t}) = \sum_{n=0}^{\infty} \tilde{\mathcal{A}}_n \tilde{\epsilon}(\tilde{t})^n \tilde{x}^n, \quad (26)$$

$$\tilde{D}(\tilde{x}, \tilde{t}) = \sum_{n=0}^{\infty} \tilde{\mathcal{D}}_n \tilde{\epsilon}(\tilde{t})^n \tilde{x}^n, \quad (27)$$

with

$$\tilde{\mathcal{A}}_n = \tau_D \frac{L^{n-1}}{n!} a^{(n)}(x_0), \quad (28)$$

$$\tilde{\mathcal{D}}_n = \frac{L^n}{n!} \frac{D^{(n)}(x_0)}{D(x_0)}, \quad (29)$$

where a superscript (n) denotes the n -th derivative with respect to x , i.e. $a^{(n)} \equiv \partial_x^n a$, $D^{(n)} \equiv \partial_x^n D$. We note that from Eq. (29) we have $\tilde{\mathcal{D}}_0 \equiv 1$.

We substitute the power series expansions Eqs. (23), (26), (27), into the dimensionless FP Eq. (15), and demand that the resulting equation hold at each power of $\tilde{\epsilon}$ separately. This yields a hierarchy of equations, which at order $\tilde{\epsilon}^k$ is given by

$$\partial_{\tilde{x}}^2 \tilde{\mathcal{Q}}_k - \tilde{x} \partial_{\tilde{x}} \tilde{\mathcal{Q}}_k - k \tilde{\mathcal{Q}}_k \quad (30)$$

$$= \sum_{l=0}^{k-1} \tilde{\mathcal{A}}_l \tilde{\mathcal{L}}_{\mathcal{A},l} \tilde{\mathcal{Q}}_{k-1-l} - \sum_{l=1}^k \tilde{\mathcal{D}}_l \tilde{\mathcal{L}}_{\mathcal{D},l} \tilde{\mathcal{Q}}_{k-l}.$$

Here, we define the sums on the right-hand side as zero if the upper summation bound is smaller than the lower summation bound, and the linear differential operators $\tilde{\mathcal{L}}_{\mathcal{A},l}$, $\tilde{\mathcal{L}}_{\mathcal{D},l}$ are given by

$$\tilde{\mathcal{L}}_{\mathcal{A},l} \tilde{\mathcal{Q}}_{k-1-l} = \partial_{\tilde{x}} \left(\tilde{x}^l \tilde{\mathcal{Q}}_{k-1-l} \right) - \tilde{x}^{l+1} \tilde{\mathcal{Q}}_{k-1-l}, \quad (31)$$

$$\begin{aligned} \tilde{\mathcal{L}}_{\mathcal{D},l} \tilde{\mathcal{Q}}_{k-l} &= \partial_{\tilde{x}}^2 \left(\tilde{x}^l \tilde{\mathcal{Q}}_{k-l} \right) - 2\tilde{x} \partial_{\tilde{x}} \left(\tilde{x}^l \tilde{\mathcal{Q}}_{k-l} \right) \\ &\quad + \tilde{x}^l (\tilde{x}^2 - 1) \tilde{\mathcal{Q}}_{k-l}. \end{aligned} \quad (32)$$

Since on the right-hand side of Eq. (30) only the $\tilde{\mathcal{Q}}_l$ with $l < k$ appear, we can solve the equation for $\tilde{\mathcal{Q}}_k$ recursively for ascending k . In App. (A 1) we provide a recursive solution approach to Eq. (30), and prove that $\tilde{\mathcal{Q}}_k$ is a

polynomial in \tilde{x} of order at most $3k$. Since \tilde{Q}_k is a polynomial and $\tilde{P}^{(0)}$ is a Gaussian, the boundary conditions Eq. (25) are fulfilled for every k .

The lowest order expressions for \tilde{Q}_k we derive are

$$\tilde{Q}_0 = 1, \quad (33)$$

$$\tilde{Q}_1 = \frac{\tilde{x}}{4} (2\tilde{A}_0 - 3\tilde{D}_1 + \tilde{D}_1\tilde{x}^2), \quad (34)$$

$$\begin{aligned} \tilde{Q}_2 = & \left(\frac{\tilde{A}_0^2}{8} + \frac{\tilde{A}_1}{4} \right) (\tilde{x}^2 - 1) + \frac{\tilde{A}_0\tilde{D}_1}{8} (\tilde{x}^4 - 5\tilde{x}^2 + 2) \\ & + \frac{\tilde{D}_1^2}{32} (\tilde{x}^6 - 11\tilde{x}^4 + 21\tilde{x}^2 - 3) + \frac{\tilde{D}_2}{12} (2\tilde{x}^4 - 9\tilde{x}^2 + 3). \end{aligned} \quad (35)$$

In our python module PySTFP [45] we include the symbolic expressions for $\tilde{Q}_0, \tilde{Q}_1, \dots, \tilde{Q}_8$, as well as code to solve Eq. (30) recursively to arbitrary desired order.

To use the perturbative solution Eq. (22) in practice, we truncate the infinite power series at a finite number of terms $K \in \mathbb{N}_0$, to get

$$\tilde{P}_K(\tilde{x}, \tilde{t}) = P^{(0)}(\tilde{x}) \left[\sum_{n=0}^K \tilde{\epsilon}^n(\tilde{t}) \tilde{Q}_n(\tilde{x}) \right] + \mathcal{O}(\tilde{\epsilon}^{K+1}), \quad (36)$$

where from the definition of $\tilde{\epsilon}$ we have $\tilde{\epsilon}^{K+1} \sim \Delta t^{(K+1)/2}$.

In App. A we show that in the form Eq. (22), our perturbative solution of the FPE conserves probability exactly, i.e. that

$$\int_{-\infty}^{\infty} d\tilde{x} \tilde{P}_K(\tilde{x}, \tilde{t}) = 1 \quad (37)$$

for any K . We therefore refer to Eq. (36) as the normalization-preserving propagator (NPP).

B. Positivity-preserving propagator

While the NPP Eq. (36) conserves probability exactly, for large enough $\tilde{\epsilon}$, \tilde{x} it can violate the non-negativity condition

$$\tilde{P}(\tilde{x}, \tilde{t}) \geq 0, \quad (38)$$

which any continuous probability density needs to fulfill.

We can rewrite Eq. (36) in a form that is manifestly positive by expressing the sum of the $\tilde{\epsilon}^k \tilde{Q}_k$ in Eq. (36) in exponential form, as

$$\begin{aligned} \tilde{P}_K(\tilde{x}, \tilde{t}) = & \frac{1}{\sqrt{2\pi}} \exp \left\{ -\frac{\tilde{x}^2}{2} \right. \\ & \left. + \ln \left[1 + \sum_{n=1}^K \tilde{\epsilon}^n(\tilde{t}) \tilde{Q}_n(\tilde{x}) + \mathcal{O}(\tilde{\epsilon}^{K+1}) \right] \right\}, \end{aligned} \quad (39)$$

where we use Eqs. (24), (33). Using the Taylor series of $\ln(1+z)$ around $z=0$,

$$\ln(1+z) = -\sum_{m=1}^K \frac{(-z)^m}{m} + \mathcal{O}(z^{K+1}), \quad (40)$$

we further rewrite the exponent in Eq. (39) as

$$\begin{aligned} \tilde{P}_K(\tilde{x}, \tilde{t}) = & \frac{1}{\sqrt{2\pi}} \exp \left\{ -\frac{\tilde{x}^2}{2} - \sum_{m=1}^K \frac{1}{m} \left[-\sum_{n=1}^K \tilde{\epsilon}^n(\tilde{t}) \tilde{Q}_n(\tilde{x}) \right]^m \right. \\ & \left. + \mathcal{O}(\tilde{\epsilon}^{K+1}) \right\}. \end{aligned} \quad (41)$$

This expression can be evaluated to any desired order $\tilde{\epsilon}^K$ in the exponent. As an exponential it is manifestly positive, so that we refer to Eq. (41) as the positivity-preserving propagator (PPP).

The NPP Eq. (36) and the PPP Eq. (41) are only equivalent to order $\tilde{\epsilon}^K$ for small enough $\tilde{\epsilon}$, since Eq. (40) only converges for $|z| < 1$. Beyond this, the two representations of the perturbative solution have different properties. Equation (36) preserves probability exactly, but can violate the condition that a probability density is always nonnegative, Eq. (38). On the other hand, Eq. (41) is manifestly positive, but in general does not exactly preserve the probability normalization.

Even more, the PPP Eq. (41) can violate the boundary conditions Eq. (20). This is because the exponent in Eq. (41) is a polynomial in \tilde{x} , which for large $|\tilde{x}|$ will be dominated by its highest power. Depending on the diffusivity D , drift a , and initial condition x_0 , the prefactor of this highest power in \tilde{x} might be such that the exponent in Eq. (41) approaches positive infinity as $\tilde{x} \rightarrow \infty$ or $\tilde{x} \rightarrow -\infty$, so that $\tilde{P} \rightarrow \infty$ in that limit. In App. B we discuss this point further, using explicit second-order perturbation theory results.

Both issues (violating nonnegativity and violating normalization) only manifest themselves for values of Δx , Δt , where our perturbation theory breaks down. Nonetheless, depending on the context it is beneficial to choose either of the forms Eq. (36), (41). In particular, as we discuss in Sect. V below, to calculate expectation values of observables it is preferable to use the NPP Eq. (36).

C. Breakdown of the perturbative solution

Our power series ansatz Eq. (22) is based on perturbing around a free-diffusion solution. For very large drift or quickly varying diffusivity profile we therefore expect that a large number of terms are needed to achieve a given accuracy for the perturbative short-time propagator.

More generally, we expect the perturbation ansatz Eq. (22) to break down once the perturbation parameter $\tilde{\epsilon}$ is not small anymore, i.e. once $\tilde{\epsilon} \gtrsim 1$. We therefore estimate the breakdown time Δt_b of our perturbative ansatz via $\tilde{\epsilon}(\tilde{t} = \Delta t_b/\tau_D) = 1/2$, which according to Eq. (16) is equivalent to

$$\frac{\Delta t_b}{\tau_D} = \frac{1}{8}. \quad (42)$$

D. L^1 -error for propagator

We now quantify the quality of a normalization-preserving approximation of the exact propagator. We only consider the NPP here because it readily allows us to evaluate expectation value integrals perturbatively, since the integrand is a product of a Gaussian and a polynomial. By contrast, the PPP leads to non-Gaussian exponentials which, as we discussed in Sect. IV B, might not even be normalizable. For our numerical example in Sect. VI below, we in App. B also discuss the errors for the PPP, both in the form Eq. (41) and for a midpoint-discretization scheme.

To measure how well an exact probability density P^e is approximated by an estimate probability density P , we consider the L^1 -error $E(\Delta t | x_0)$. This error is defined as

$$E(\Delta t | x_0) \equiv \|P - P^e\|_1 \equiv \int_{-\infty}^{\infty} dx E_p(x, \Delta t | x_0), \quad (43)$$

where the pointwise error E_p of the continuous probability densities we consider is given by

$$E_p(x, \Delta t | x_0) \equiv |P(x, t | x_0, t_0) - P^e(x, t | x_0, t_0)|. \quad (44)$$

By direct substitution, the error estimates Eq. (11) of the GP and Eq. (36) of the NPP yield the corresponding scaling of the L^1 errors Eq. (43), i.e.

$$E_{\text{GP}}(\Delta t | x_0) \sim \Delta t^{\beta-1/2}, \quad (45)$$

$$E_{\text{NPP}}(\Delta t | x_0) \sim \Delta t^{(K+1)/2}, \quad (46)$$

where as before $\beta = 1$ for multiplicative noise and $\beta = 3/2$ for additive noise, and the integer K is the truncation order in Eq. (36). Note that Eq. (45) shows that, in general, the GP approximates the true transition density only to sublinear order in the time increment Δt .

V. OBSERVABLES

A. Moments

The NPP Eq. (23) allows us to evaluate any expectation value perturbatively. For example, for $n \in \mathbb{N}_0$ we obtain a perturbation series for the n -th moment as

$$\langle \Delta x^n \rangle = R^n \langle \tilde{x}^n \rangle = R^n \sum_{k=0}^{\infty} \tilde{\epsilon}^k \langle \tilde{x}^n \rangle^{(k)} \quad (47)$$

$$= R^n \sum_{\substack{k=0 \\ k+n \text{ even}}}^{\infty} \tilde{\epsilon}^k \langle \tilde{x}^n \rangle^{(k)}, \quad (48)$$

where

$$\langle \tilde{x}^n \rangle^{(k)} \equiv \int_{-\infty}^{\infty} d\tilde{x} \tilde{x}^n \tilde{Q}_k(\tilde{x}) \tilde{P}^{(0)}(\tilde{x}), \quad (49)$$

and where we use that $\langle \tilde{x}^n \rangle^{(k)} = 0$ whenever $n+k$ is odd, as shown in App. A 2. The form of Eq. (49) demonstrates why for the moments it is preferable to use the NPP over the PPP. Namely, the integral in Eq. (49) is a product of a polynomial in \tilde{x} and a Gaussian, which can readily be evaluated analytically via repeated integration by parts. On the other hand, the evaluation of expectation value integrals using the PPP Eq. (41) is not as straightforward, for example since the truncated PPP need not even be normalizable.

Since $R \sim \tilde{\epsilon} \sim \Delta t^{1/2}$, it follows from Eq. (48) that

$$\langle \Delta x^n \rangle = \begin{cases} \mathcal{O}(\Delta t^{n/2}) & n \text{ even,} \\ \mathcal{O}(\Delta t^{(n+1)/2}) & n \text{ odd,} \end{cases} \quad (50)$$

so that to linear order in Δt , the only nonvanishing moments are $\langle \Delta x^0 \rangle \equiv 1$, $\langle \Delta x \rangle$, $\langle \Delta x^2 \rangle$; this is of course required by the Pawula Theorem [2, 52].

Using our NPP to order K , we can evaluate the n -th moment perturbatively. More explicitly, substituting Eq. (36) into the series Eq. (48), we obtain

$$\langle \Delta x^n \rangle = R^n \left[\sum_{\substack{k=0 \\ k+n \text{ even}}}^K \tilde{\epsilon}^k \langle \tilde{x}^n \rangle^{(k)} + \mathcal{O}(\tilde{\epsilon}^\gamma) \right]. \quad (51)$$

where $\gamma = K+1$ if $n+K$ is odd, and $\gamma = K+2$ if $n+K$ is even. Recalling that $R \sim \tilde{\epsilon} \sim \Delta t^{1/2}$, we thus have that

$$\langle \Delta x^n \rangle = R^n \sum_{\substack{k=0 \\ k+n \text{ even}}}^K \tilde{\epsilon}^k \langle \tilde{x}^n \rangle^{(k)} \quad (52)$$

$$+ \begin{cases} \mathcal{O}(\Delta t^{(n+K+2)/2}) & \text{if } n+K \text{ even,} \\ \mathcal{O}(\Delta t^{(n+K+1)/2}) & \text{if } n+K \text{ odd.} \end{cases}$$

Using Eq. (49) we can evaluate each moment to any desired order, once the necessary polynomials $\tilde{Q}_k(\tilde{x})$ have been derived using the recursive scheme from Sect. IV A; in App. C, we print the resulting perturbation expansions of $\langle \Delta x^n \rangle$ to order Δt^3 for $n = 0, 1, 2, 3$. In the module PySTFP we provide analytical expressions for the moments $\langle \Delta x^n \rangle$ for $n = 0, 1, \dots, 4$ up to errors of the order Δt^5 [45].

B. Finite-time Kramers-Moyal coefficients

From Eq. (52), we in particular obtain finite-time generalizations to the Kramers-Moyal coefficients. To lead-

ing orders these follow as

$$\begin{aligned}\alpha_1(x_0, \Delta t) &\equiv \frac{\langle \Delta x \rangle}{\Delta t} \\ &= a + \frac{\Delta t}{2} [a \partial_x a + D \partial_x^2 a] + \mathcal{O}(\Delta t^2),\end{aligned}\quad (53)$$

$$\begin{aligned}\alpha_2(x_0, \Delta t) &\equiv \frac{\langle \Delta x^2 \rangle}{\Delta t} \\ &= 2D + \Delta t [a^2 + a \partial_x D + 2(\partial_x a)D + D \partial_x^2 D] \\ &\quad + \mathcal{O}(\Delta t^2),\end{aligned}\quad (54)$$

where a , D , and their derivatives are evaluated at x_0 . From Eqs. (53), (54) it is apparent that in the limit $\Delta t \rightarrow 0$, the usual Kramers-Moyal coefficients [2, 3] are recovered. According to Eqs. (53), (54) the first two moments both scale as Δt to leading order, which is in agreement with Eq. (50). Our Eqs. (53), (54) are identical to those previously derived in the literature [53–55].

C. Medium entropy production rate

As another observable, we now consider the ensemble medium entropy production [13, 34, 56]

$$\dot{S}^m(t) \equiv \int_{-\infty}^{\infty} dx \frac{j(x,t)}{D(x)} [a(x) - (\partial_x D)(x)], \quad (55)$$

with the standard FP probability flux

$$j \equiv aP - \partial_x(DP). \quad (56)$$

Physically speaking, the ensemble medium entropy production Eq. (55) describes the rate at which the reaction coordinate dissipates energy into the heat bath [34] (which is modeled via the random force term in the Itô-Langevin Eq. (4)).

As we discuss in detail in App. D, by substituting our perturbative propagator Eq. (23) into Eq. (55) we obtain a short-time perturbation series for \dot{S}^m . To leading order we have

$$\dot{S}^m = \frac{1}{D} (a - \partial_x D)^2 + \partial_x a - \partial_x^2 D + \mathcal{O}(\Delta t), \quad (57)$$

where a , D and their derivatives are evaluated at x_0 . In our python module PySTFP [45] we give the symbolic expression for \dot{S}^m up to order Δt^4 .

For systems that allow for a zero-flux steady state, which includes (non-periodic) one-dimensional systems with a drift that confines the particle to a finite spatial domain, we in App. E recall that the physical interpretation of Eq. (55) can be made more explicit [56, 57]. Briefly, for such systems we can define a potential U such that the steady state is a Boltzmann distribution with respect to U . The medium entropy production Eq. (55) can then be rewritten in terms of U as [56, 57]

$$\dot{S}^m(t) = -\partial_t \langle U \rangle, \quad (58)$$

i.e. as the negative rate of change of the mean potential (internal energy) of the system. Since any change in potential has to happen through exchange of energy with the heat bath, we can interpret Eq. (57) equivalently as describing the mean loss in internal energy, or the mean energy dissipated into the heat bath [34, 56, 57].

While we consider the medium entropy production rate here, we in App. D provide perturbative evaluations of the Gibbs entropy, as well as the total entropy production rate, from the stochastic thermodynamics literature [13, 34].

D. Error for expectation values

For a general observable $f(x, t, x_0, t_0)$ we consider the error in the instantaneous expectation value, defined by

$$E_f(\Delta t | x_0) \equiv |\langle f \rangle - \langle f \rangle^e|, \quad (59)$$

where

$$\langle f \rangle \equiv \int_{-\infty}^{\infty} dx f(x, t, x_0, t_0) P(x, t | x_0, t_0), \quad (60)$$

$$\langle f \rangle^e \equiv \int_{-\infty}^{\infty} dx f(x, t, x_0, t_0) P^e(x, t | x_0, t_0). \quad (61)$$

with P , P^e the approximate and exact propagator, respectively.

For the error Eq. (59) we first consider the special case where $f \equiv \langle \Delta x^n \rangle$ for some positive integer n . From Eq. (52) we then obtain that for the NPP at order K it holds that

$$E_{\text{NPP}, \langle \Delta x^n \rangle}(\Delta t | x_0) \sim \begin{cases} \Delta t^{(n+K+2)/2} & \text{if } n+K \text{ even,} \\ \Delta t^{(n+K+1)/2} & \text{if } n+K \text{ odd.} \end{cases} \quad (62)$$

Thus, for the first two finite-time Kramers-Moyal coefficients we have

$$E_{\text{NPP}, \alpha_1}(\Delta t | x_0) \sim \begin{cases} \Delta t^{(K+1)/2} & \text{if } K \text{ odd,} \\ \Delta t^{K/2} & \text{if } K \text{ even,} \end{cases} \quad (63)$$

$$E_{\text{NPP}, \alpha_2}(\Delta t | x_0) \sim \begin{cases} \Delta t^{K/2+1} & \text{if } K \text{ even,} \\ \Delta t^{(K+1)/2} & \text{if } K \text{ odd,} \end{cases} \quad (64)$$

where α_1 , α_2 are defined by Eqs. (53), (54), and where we use the perturbative expectation values from Eq. (52).

For a general analytical function f , the expectation value $\langle f \rangle$ can be related to the moments Eq. (48) via a two-dimensional Taylor expansion of f around $(x, t) = (x_0, t_0)$. For example, to calculate $\langle f \rangle$ to linear order in the timestep, we obtain

$$\begin{aligned}\langle f \rangle &= f + (\partial_x f) \langle \Delta x \rangle + \frac{\partial_x^2 f}{2} \langle \Delta x^2 \rangle \\ &\quad + (\partial_t f) \Delta t + \langle \mathcal{O}(\Delta x^3) \rangle + \mathcal{O}(\Delta t^2),\end{aligned}\quad (65)$$

where f and its derivatives on the right-hand side are all evaluated at $(x, t, x_0, t_0) = (x_0, t_0, x_0, t_0)$ and where we use that the NPP conserves probability exactly. Using Eqs. (53), (54), (50) we get an explicit expression for Eq. (65) in terms of diffusivity and drift as

$$\langle f(\Delta x, \Delta t, x_0) \rangle = f + \Delta t [a\partial_x f + D\partial_x^2 f + \partial_t f] + \mathcal{O}(\Delta t^2), \quad (66)$$

where a , D , f and its derivatives are evaluated at $(x, t) = (x_0, t_0)$.

Similarly, higher-order approximations to $\langle f \rangle$ are obtained by higher-order Taylor expansion of f and subsequent perturbative calculation of the moments $\langle \Delta x^n \rangle$ that emerge from the Taylor expansion. We now discuss how to evaluate the expectation value $\langle f \rangle$ up to an error of order $\Delta t^{\alpha+1}$, i.e. to accuracy Δt^α . From Eq. (50) we see that only the moments $\langle \Delta x^0 \rangle \equiv 1$, $\langle \Delta x^1 \rangle$, ..., $\langle \Delta x^{2\alpha} \rangle$ contribute to any expression at order Δt^α ; we therefore need to Taylor expand f up to order 2α . For a fixed order K of the NPP, the errors of the moments $\langle \Delta x^0 \rangle \equiv 1$, $\langle \Delta x \rangle$, $\langle \Delta x^2 \rangle$, ..., $\langle \Delta x^{2\alpha} \rangle$ are then given by Eq. (62). Among the relevant moments, the worst accuracy is realized by the first moment, $\langle \Delta x \rangle$. In fact, from Eq. (62) it follows that, to obtain $\langle \Delta x \rangle$ with an error that scales as $\Delta t^{\alpha+1}$, we need $K \geq \alpha$. Summing up, to calculate $\langle f \rangle$ up to an error that scales as $\Delta t^{\alpha+1}$, we need to consider the spatial Taylor expansion of f up to order $\Delta t^{2\alpha}$, and need to know the NPP to order at least $K = \alpha$ to evaluate the expectation values. Equation (66) represents the case $\alpha = 1$, where we needed to consider the first and the second moment (since $2\alpha = 2$), and where we need to know the NPP to order at least $K = \alpha = 1$ to evaluate the expectation values.

To estimate the error in expectation value for the GP Eq. (11), we first note that from direct calculation we have that this propagator predicts the first two moments as $\langle \Delta x \rangle_{\text{GP}} = a(x_0)\Delta t$, $\langle \Delta x^2 \rangle_{\text{GP}} = 2D(x_0)\Delta t + (\partial_x a)^2 \Delta t^2$. Upon comparison with Eqs. (53), (54), we conclude that for $n = 1, 2$ we have

$$E_{\text{GP}, \langle \Delta x^n \rangle}(\Delta t | x_0) \sim \Delta t^2. \quad (67)$$

Consequently, we obtain the corresponding error in the first two finite-time Kramers-Moyal coefficients as

$$E_{\text{GP}, \alpha_n}(\Delta t | x_0) \sim \Delta t. \quad (68)$$

From Eqs. (65), (67), we furthermore conclude that for the GP and an analytical function f it in general holds that

$$E_{\text{GP}, f}(\Delta t | x_0) \sim \Delta t^2. \quad (69)$$

Note that this scaling is not in contradiction with Eq. (68); this is because α_1 , α_2 are not analytic functions in Δt , and thus cannot be represented in the form Eq. (65).

Equations (45), (69) demonstrate that, while for a general Itô-Langevin equation with multiplicative noise the

error in the GP Eq. (11) scales to leading order as $\Delta t^{1/2}$, this propagator is still sufficient to evaluate expectation values with order- Δt accuracy.

VI. NUMERICAL EXAMPLE

A. System

For the length scale L and a time scale T , we now consider an explicit example system. As explained in more detail in App. F, we construct diffusivity and drift profiles such that we can evaluate the analytical propagator exactly. We show the resulting diffusivity and drift profiles in Fig. 1. Unless stated otherwise we in the following consider the initial condition $x_0/L = 0.5$, which is shown in Fig. 1 as vertical gray dashed line. For the diffusivity, drift, and initial position that we consider here the breakdown lagtime Eq. (42) evaluates to $\Delta t_b/T \approx 0.10$,

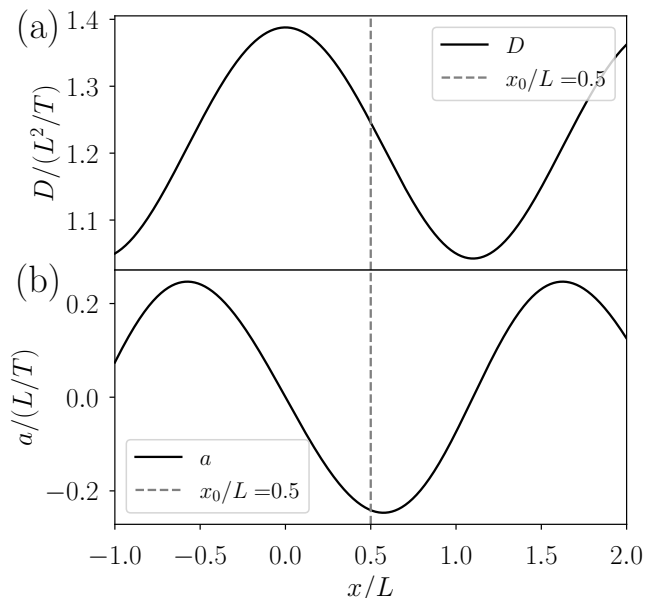


Figure 1. **Diffusivity and drift profile for the numerical example in Sect. VI.** The black lines show the (a) diffusivity and (b) drift profile defined in App. F as a function of the position x . The vertical dashed line denotes the initial position of the particle for which we consider the short-time propagator.

B. Normalization-preserving propagator

In Fig. 2, we compare the exact propagator (black solid line) with both the GP Eq. (11) (red dashed line), and our NPP Eq. (36) to order $\epsilon^2 \sim \Delta t$ ($K = 2$, blue dotted line) and $\epsilon^8 \sim \Delta t^4$ ($K = 8$, green dash-dotted line).

In Fig. 2 (a) we show the three perturbative solutions together with the exact analytical solution for $\Delta t/T =$

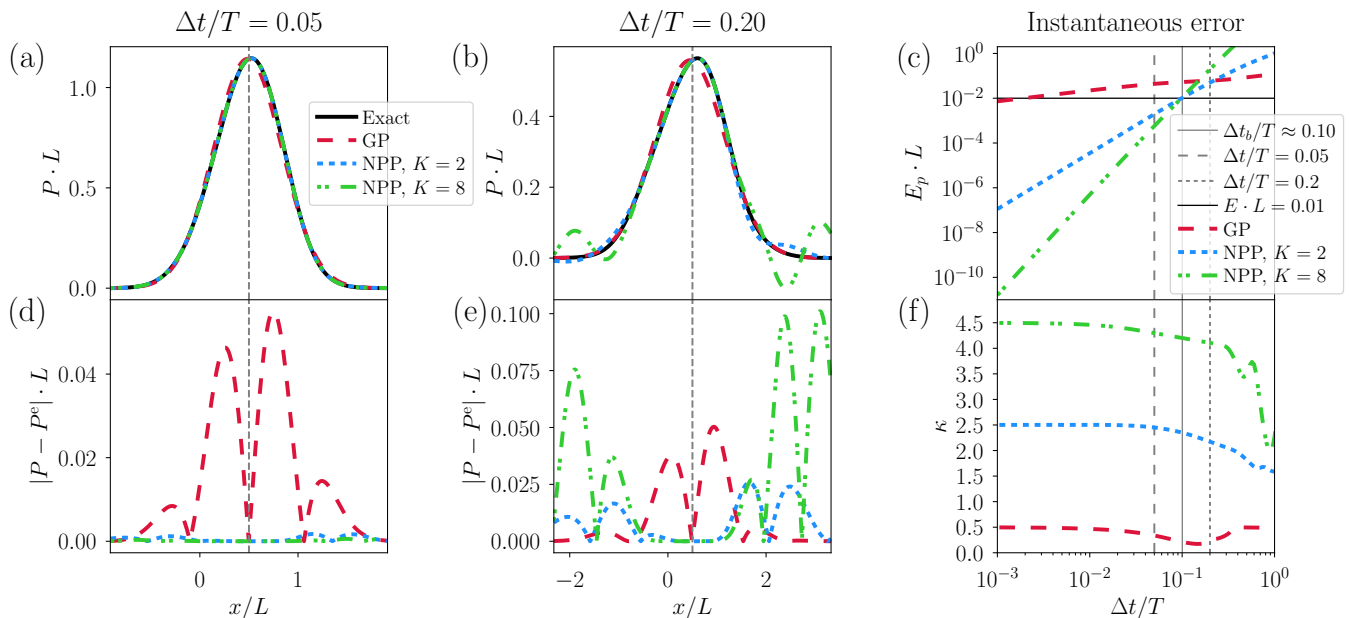


Figure 2. **Comparison of exact Fokker-Planck solution with various approximate solutions.** Throughout this figure, data pertaining to the Gaussian propagator (GP) Eq. (11) is shown as red dashed line; data pertaining to the normalization-preserving propagator (NPP) Eq. (36) is shown for $K = 2$ as blue dash-dotted lines, and for $K = 8$ as a green dotted lines. For all data we use the drift and diffusivity from Fig. 1, as well as the initial condition $x_0/L = 0.5$. In subplots (a), (b) we plot the exact solution P^e to the FP Eq. (1) (black solid line), as well as various approximations. In subplots (d), (e) we plot the respective pointwise error of the approximate propagators, as defined in Eq. (44). While in subplots (a), (d) we consider propagators for the lagtime $\Delta t/T = 0.05$, in subplots (b), (e) we consider $\Delta t/T = 0.2$. The legend from subplot (a) is valid for subplots (a), (b), (d), (e). In subplot (c) we show the L^1 error Eq. (43) of the approximate propagators as a function of the lagtime $\Delta t/T$; in subplot (f) we plot the corresponding local exponents Eq. (71). The vertical lines in subplots (c), (f) indicate the lagtimes used for subplots (a), (b), (d), (e), as well as the breakdown time $\Delta t_b/T \approx 0.10$ defined via Eq. (42). The horizontal line in subplot (c) indicates the error value $E_p \cdot L = 0.01 = 1\%$.

0.05, i.e. for a time shorter than the breakdown time Δt_b . We observe that for $\Delta t/T = 0.05$ all perturbative solutions agree well with the analytical solution on the scales used for the plot. In Fig. 2 (d) we show the pointwise error Eq. (44) of the three perturbative solutions. Consistent with subplot (a) we see that all pointwise errors are small compared to the typical values of the densities. On the other hand, the pointwise error for the GP is almost one order of magnitude larger than the pointwise error of the NPP with $K = 2$. The pointwise errors of both the GP and the NPP with $K = 2$ are significantly larger than the pointwise error in the NPP with $K = 8$, which on the scales used for Fig. 2 (d) seems insignificant. Consistent with these observations, the integrated pointwise errors Eq. (43) are given by $E_{\text{GP}} \approx 0.0531$ (GP), $E_{\text{NPP}} \approx 0.0088$ (NPP, $K = 2$), and $E_{\text{NPP}} \approx 0.0006$ (NPP, $K = 8$).

In Fig. 2 (b) we plot the perturbative and exact propagator for $\Delta t = 0.2T$, which is approximately twice the breakdown time Δt_b . We observe that now all approximate propagators deviate visibly from the exact analytical solution. While the GP deviates at the center of the distribution ($x/L \approx 0$), the deviations in the NPPs occur at the tails ($x/L \approx \pm 2$). We confirm this in

Fig. 2 (e), where we show the pointwise error Eq. (44) for $\Delta t/T = 0.2$. We see that now the maximal error occurs in the NPP with $K = 8$ at around $x/L \approx \pm 2$, where we observe oscillations in the solution in Fig. 2 (b). The corresponding integrated pointwise errors Eq. (43), evaluated at $\Delta t/T = 0.2$, $x_0/L = 0.5$, follow as $E_{\text{GP}} \approx 0.06$ (GP), $E_{\text{NPP}} \approx 0.05$ (NPP, $K = 2$), and $E_{\text{NPP}} \approx 0.19$ (NPP, $K = 8$).

In Fig. 2 (c) we show the instantaneous L^1 -error Eq. (43) of the perturbative propagators as a function of the time increment Δt ; we indicate the values $\Delta t/T = 0.05, 0.2$ from the left and middle column of Fig. 2 as vertical broken lines, and the breakdown time $\Delta t_b/T \approx 0.10$ as a vertical solid line. We observe that for the smallest lagtime considered, $\Delta t/T = 10^{-3}$, the error in the GP Eq. (11) is about five orders of magnitude larger than the error of the NPP at order $\tilde{\epsilon}^2 \sim \Delta t$, and about nine orders of magnitude larger than the error of the NPP at order $\tilde{\epsilon}^8 \sim \Delta t^4$. As the lagtime Δt is increased, all errors display their respective expected power law scaling

$$E(\Delta t, x_0) \sim \Delta t^{\gamma+1/2}, \quad (70)$$

where γ is the order of accuracy for the solution; while for the GP Eq. (11) this is $\gamma = 0$, for the NPP Eq. (22) with

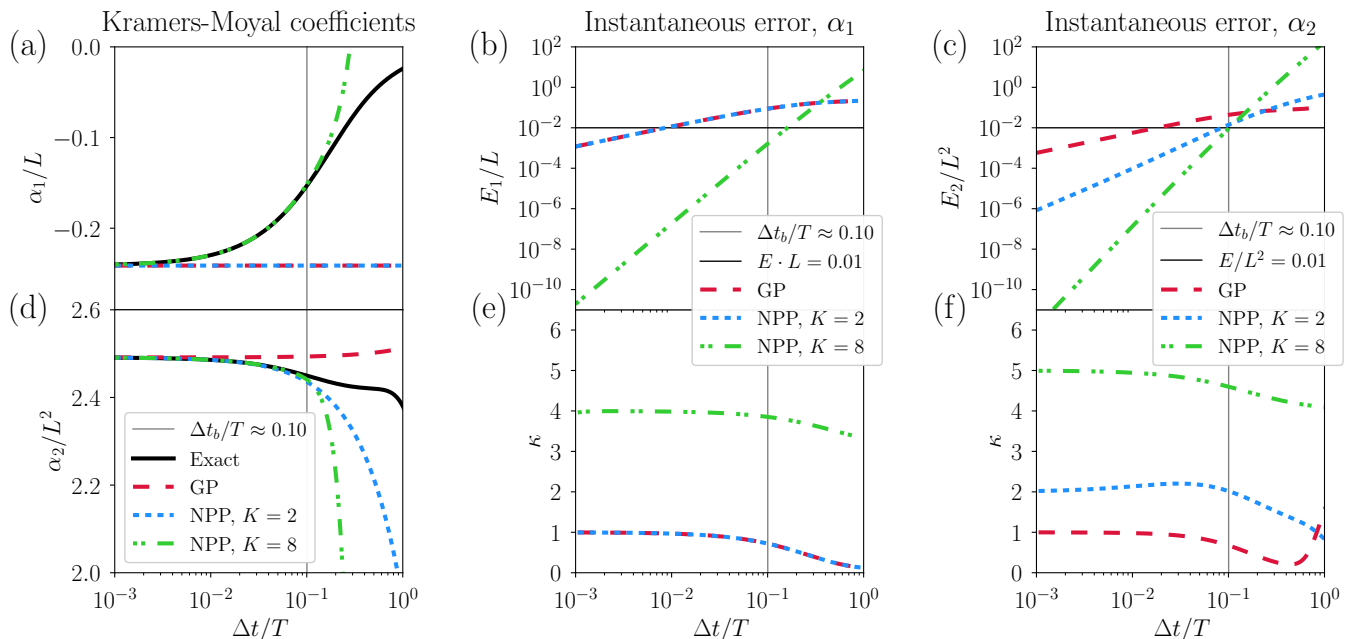


Figure 3. **Comparison of exact finite-time Kramers-Moyal coefficients with various approximations.** Throughout this figure, data pertaining to the Gaussian propagator (GP) Eq. (11) is plotted as red dashed line; data pertaining to the normalization-preserving propagator (NPP) Eq. (36) with $K = 2$ is shown as blue dotted line, and with $K = 8$ as green dash-dotted line. We show the (a) first and (d) second exact finite-time Kramers-Moyal coefficients as black solid lines, together with various approximations. The legend in (d) is also valid for (a). While in (b), (c) we show the instantaneous error Eq. (72) for the approximate finite-time Kramers-Moyal coefficients as a function of the lagtime $\Delta t/T$, in (e), (f) we plot the corresponding running exponents Eq. (71). In all subplots, the vertical solid line indicates the breakdown time $\Delta t_b/T \approx 0.10$ defined in Eq. (42).

order of the perturbation theory K we have $\gamma = K/2$. To make the scalings more explicit we in Fig. 2 (f) plot the running exponent

$$\kappa(\Delta t) \equiv \frac{\partial \ln(E)}{\partial \ln(\Delta t)}, \quad (71)$$

which is defined such that if $E \sim \Delta t^\alpha$ for some real number α , it holds that $\kappa = \alpha$. Figure 2 (f) vividly demonstrates all anticipated power law scalings of the error for small $\Delta t \ll \Delta t_b$. As the time increment is increased to $\Delta t \approx \Delta t_b$, all errors start to deviate from their respective power law scaling and, as Fig. 2 (c) shows, become of the order $E \cdot L \approx 0.01 = 1\%$. For times larger than the breakdown time, the NPP at order $\tilde{\epsilon}^8 \sim \Delta t^4$ starts to perform worse as compared to the lower-order propagators; this is consistent with Fig. 2 (e). We speculate that the higher-order NPP performs worse beyond the breakdown of perturbation theory because of the higher polynomial order of the \tilde{Q}_k (the polynomial order increases as $3k$); these high-order polynomials may result in very uncontrolled behavior.

To summarize, Fig. 2 shows that for small enough lagtime the NPP with $K = 8$ significantly outperforms both the NPP with $K = 2$, as well as the GP Eq. (11). As the lagtime approaches the breakdown time Δt_b , all propagators approximate the exact analytical solution comparably well. For lagtimes $\Delta t > \Delta t_b$, all propagators yield an

error $E \cdot L > 0.01$, with the NPP with $K = 8$ producing the largest error out of the three propagators considered.

C. Finite-time Kramers-Moyal coefficients

We now consider the first two finite-time Kramers-Moyal coefficients Eqs. (53), (54) for our example system.

In Fig. 3 (a) we compare the exact first finite-time Kramers-Moyal coefficient as a function of the lagtime (black solid line) to approximate evaluations, based on the GP Eq. (11) (red dashed line), as well as the NPP Eq. (36) at order $\tilde{\epsilon}^2 \sim \Delta t$ ($K = 2$, blue dotted line) and $\tilde{\epsilon}^8 \sim \Delta t^4$ ($K = 8$, green dash-dotted line). We observe that the GP and the NPP with $K = 2$ lead to identical time-independent predictions, which start to deviate from the exact result at the smallest lagtimes considered, $\Delta t/T \approx 10^{-3}$. The NPP with $K = 8$ on the other hand describes the exact result well for lagtimes up to $\Delta t \approx \Delta t_b \approx 0.10T$.

To quantify the deviations between exact and perturbative Kramers-Moyal coefficients, we consider the instantaneous error

$$E_i(\Delta t, x_0) = |\alpha_i(\Delta t, x_0) - \alpha_i^e(\Delta t, x_0)|, \quad (72)$$

where α_i is the respective perturbative finite-time Kramers-Moyal coefficient, and α_i^e is the corresponding

exact result. In Fig. 3 (b) we plot the instantaneous error for the first finite-time Kramers-Moyal coefficient, for which $i = 1$ in Eq. (72). In subplot (e) we show the corresponding local exponent Eq. (71). Consistent with subplot (a), in subplot (b) we see that the instantaneous errors for GP and NPP with $K = 2$ are identical. According to Fig. 3 (e), both errors scale as $E_1 \sim \Delta t$, which confirms our error estimates Eqs. (63), (68). Figure 3 (b) shows that for $\Delta t \lesssim \Delta t_b$, the error of the NPP with $K = 8$ is typically orders of magnitude smaller than the errors of the GP and of the NPP with $K = 2$. In Fig. 3 (e) we observe a local exponent $\kappa = 4$ for the NPP with $K = 8$, which is in agreement with Eq. (63).

In Fig. 3 (d) we show plots of the second finite-time Kramers-Moyal coefficient Eq. (54). Contrary to subplot (a), in subplot (d) the GP and NPP with $K = 2$ are not identical. While the GP starts to visibly deviate from the exact result at $\Delta t/T \approx 0.01$, the NPP with $K = 2$ describes the exact result on the plotting scales up to $\Delta t/T \approx 0.1$. At around the same lagtime, also the NPP with $K = 8$ starts to visibly deviate from the exact result. In Fig. 3 (c) we show the instantaneous error Eq. (72) for $i = 2$. We see that all approximate propagators lead to different power law scalings; according to Fig. 3 (f) the respective power law exponents of the errors are $\kappa = 1$ (GP), $\kappa = 2$ (NPP, $K = 2$), and $\kappa = 5$ (NPP, $K = 8$). These scalings are all consistent with our estimates Eqs. (64), (68).

In summary, Fig. 3 shows that both the GP and the NPP with $K = 2$ predict the first two finite-time Kramers-Moyal coefficients only up to lagtimes that are significantly smaller than Δt_b . In comparison, Fig. 3 (b), (c) shows that the pointwise error our NPP with $K = 8$ is typically orders of magnitude smaller, and for $\Delta t < \Delta t_b$ is always less than 1%. All power laws observed in Fig. 3 are in agreement with our error estimates from Sect. V D.

D. Medium entropy production rate

We now turn to the medium entropy production rate Eq. (55). In Fig. 4 (a) we compare the exact medium entropy production rate (black solid line) with approximations based on the GP Eq. (11) (red dashed line), as well as the NPP at order $\tilde{\epsilon}^2 \sim \Delta t$ ($K = 2$, blue dotted line) and at order $\tilde{\epsilon}^8 \sim \Delta t^4$ ($K = 8$, green dash-dotted line). We see that for $\Delta t/T < 10^{-2}$, all approximations describe the exact results very well on the plotting scales. We confirm this in Fig. 4 (b), where we plot the instantaneous relative error

$$E_{\text{rel}}(\Delta t) = \left| \frac{\dot{S}^{\text{m,e}}(\Delta t) - \dot{S}^{\text{m}}(\Delta t)}{\dot{S}^{\text{m,e}}(\Delta t)} \right|, \quad (73)$$

where here $\dot{S}^{\text{m,e}}$, \dot{S}^{m} stand for the exact and approximate medium entropy production, respectively. From Fig. 4 (b) we observe that while the NPP approximation with $K = 2$ surpasses 1% relative error at $\Delta t/T \approx 7 \times 10^{-3}$,

the GP does so at $\Delta t/T \approx 1.5 \cdot 10^{-2}$, and the the $K = 8$ approximation at $\Delta t/T \approx 3.1 \cdot 10^{-2}$. Finally, in Fig. 4 (c) we show the running exponent Eq. (71) pertaining to the relative error Eq. (73). As expected, before the breakdown time Δt_b , the error for the GP and the NPP with $K = 2$ scales as Δt^2 , which for the GP is in agreement with Eqs. (69). Similarly, the error for the NPP with $K = 8$ scales as Δt^5 . Both error scalings for the NPP are anticipated, as we evaluate the perturbative medium entropy production to orders Δt (corresponding to $K = 2$) and Δt^4 (corresponding to $K = 8$).

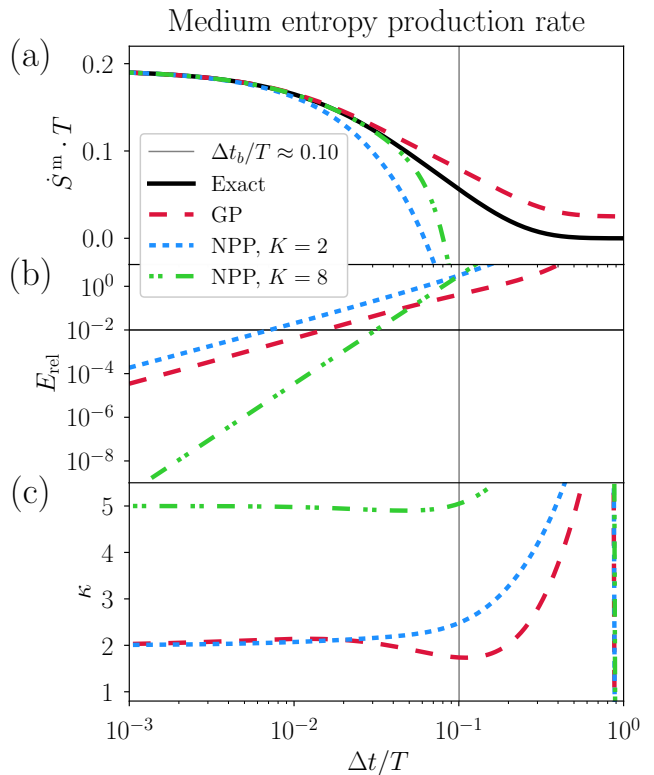


Figure 4. **Comparison of exact medium entropy production with approximations.** Throughout this figure, we plot data pertaining to the GP Eq. (11) as red dashed line, to the normalization-preserving propagator (NPP) Eq. (36) with $K = 2$ as blue dotted line, and with $K = 8$ as green dash-dotted line. The legend in (a) is also valid for (b), (c). (a) We show the exact medium entropy production rate Eq. (55) as a function of the lagtime Δt as black solid line, together with various approximation. While in (b) we show the instantaneous relative error Eq. (73) of the approximations from (a), we in (c) show the running exponent Eq. (71) of the relative error. In all subplots, the vertical solid line indicates the breakdown time $\Delta t_b/T \approx 0.10$ defined in Eq. (42).

VII. SUMMARY AND CONCLUSIONS

In this work we present a perturbation approach for evaluating the short-time Fokker-Planck propagator to in

principle arbitrary precision. We provide two representations of the resulting perturbative propagator, namely the normalization-preserving propagator (NPP) and the positivity-preserving propagator (PPP) [41, 42]. The NPP preserves the proper normalization of the propagator exactly, but can take on negative values outside of its regime of validity, i.e. for very improbable large increments $\Delta x = x - x_0$, or for time increments $\Delta t = t - t_0$ so large that our perturbation ansatz breaks down. The PPP on the other hand is manifestly positive, but in general will not preserve the proper normalization of a probability density; more so, depending on the diffusivity and drift profiles, the PPP might not even fulfill the proper boundary conditions of the underlying Fokker-Planck equation (FPE). Since it allows for straightforward calculation of expectation values, we use the NPP to evaluate perturbative expressions for the moments $\langle \Delta x^n \rangle$, the first two finite-time Kramers-Moyal coefficients, as well as the medium entropy production. We derive error estimates for both our perturbative propagators and expectation values, and compare our results to the corresponding errors of the standard Gaussian short-time propagator (GP). Remarkably, we find that the GP in general has an integrated pointwise absolute error of the order of $\sqrt{\Delta t}$, i.e. is a sublinear approximation to the true short-time propagator; still, the GP allows to evaluate expectation values with order- Δt accuracy. We illustrate all our results via an explicit numerical example, where we find that our approximation propagators can outperform the GP in terms of accuracy by orders of magnitude. However, in regimes where the perturbation theory breaks down (e.g. too large lagtimes), the error of our approximations can become worse than that of the GP; we speculate that this is due to the high-order polynomials that our perturbation theory contains.

Accurate approximations of the short-time propagator and of short-time expectation values have several applications that are fundamental to the practical use of diffusive stochastic dynamics models. One such application is the parametrization of the FPE Eq. (1) from observed time series. For this, one measures expectation values of short-time observables, such as the first two finite-time Kramers-Moyal coefficients $\langle \Delta x \rangle / \Delta t$, $\langle \Delta x^2 \rangle / \Delta t$. These coefficients are expressed in terms of drift and diffusivity via theoretical estimates such as Eqs. (53), (54), or higher-order versions thereof (which we provide in our python module [45]). The FPE is then parametrized by choosing drift and diffusivity such that the theoretical estimates reproduce the measured expectation values [5–7]. Here, more accurate theoretical estimates of the finite-time Kramers-Moyal coefficients reduce one source of error, and will be in particular relevant for time series that can only be observed with relatively low temporal frequency. The same holds true for other methods of parameter fitting, such as the maximum likelihood approach for observed transitions [20].

A related application of our short-time propagator is the numerical sampling of time-discretized path-spaces

via Markov Chain Monte Carlo (MCMC), [21, 23–26, 28]. This can be used for calculating expectation values over path ensembles, or for sampling the posterior distribution in Bayesian parameter estimation or augmentation [20, 22, 23, 28]. Here, a more accurate short-time propagator allows to use larger time increments Δt for the time-slicing discretization of the probability density on path space, which results in a lower-dimensional sampling problem.

Another possible avenue for further research is the relation between our PPP Eq. (B4) and the multiplicative-noise stochastic actions that have been derived in the literature [12, 14, 15, 17–19, 36]. For the special case of additive noise, where the diffusivity is independent of x , the PPP was recently used to discuss that the form of the path-integral action depends on whether one evaluates the action on a differentiable path (where increments scale as $\Delta x \sim \Delta t$), or a typical realization of the Itô-Langevin Eq. (4) (where increments scale as $\Delta x \sim \sqrt{\Delta t}$) [6]. For this analysis, it was critical to consider the short-time propagator to order Δt in the exponent, and so in Ref. [6] an approximation that goes beyond the usual Gaussian propagator Eq. (11) was employed. For multiplicative noise, defining and working with a path-integral action is in general more intricate [7, 17–19, 36, 58, 59]. Similarly to the result of Ref. [6] discussed above, it will be interesting to investigate whether also for the multiplicative-noise stochastic action, our PPP to order Δt (which we give explicitly to second order in perturbation theory in App. B), will lead to insights that cannot be obtained from the Gaussian propagator Eq. (11).

We here derive the short-time propagator only for a one-dimensional reaction coordinate. It is an open question whether derivation can be generalized also to multidimensional systems, for which one would perturb around a multivariate Gaussian distribution, as explored in Refs. [42, 43] by different means. The key question here will be whether the multidimensional equivalent of Eq. (30) allows for systematic solution.

ACKNOWLEDGMENTS

We thank Ronojoy Adhikari, Michael E. Cates, and Erwin Frey for many helpful discussions. Work funded in part by the European Research Council under the Horizon 2020 Programme, ERC grant agreement number 740269. We acknowledge funding from the European Union’s Horizon 2020 research and innovation programme under the Marie Skłodowska-Curie grant agreement No 101068745.

Appendix A: Derivation and properties of the perturbative solution

1. Solution of the recursive equation

We now derive a recursive scheme to solve Eq. (30), and show that the resulting solution $\tilde{Q}_k(\tilde{x})$ at order k is a polynomial in \tilde{x} of order at most $3k$. We proceed by induction.

For the base case $k = 0$ we note that $\tilde{Q}_0 = 1$ solves Eq. (30), and is a polynomial in \tilde{x} of order $3k = 0$

For the induction step we assume that for a given $k \geq 1$, each \tilde{Q}_l with $l < k$ is a known polynomial in \tilde{x} of order at most $3l$. We can then evaluate the right-hand side of Eq. (30), which results in a polynomial in \tilde{x} . By counting the highest powers of each term on the right-hand side of Eq. (30), we see that this polynomial is of order at most $3k$. More explicitly, the highest possible power in \tilde{x} is obtained from the $l = 1$ term of the second sum on the right-hand side of Eq. (30), and more specifically by the term $\tilde{x}^{l+2}\tilde{Q}_{k-l}$ in Eq. (32): For $l = 1$, and using that \tilde{Q}_{k-l} is at most of order $\tilde{x}^{3(k-l)}$, we see that the highest possible power in $\tilde{x}^{l+2}\tilde{Q}_{k-l}$ is $\tilde{x}^{l+2}\tilde{x}^{3(k-l)} = \tilde{x}^{3k}$.

We now have established that in the induction step, the right-hand side of the inhomogeneous differential Eq. (30) is a polynomial of order at most \tilde{x}^{3k} . Since the differential operator on the left-hand side of Eq. (30) is linear, we can obtain a solution for the polynomial inhomogeneity by summing over for all the possible monomials $\tilde{x}^0, \tilde{x}^1, \dots, \tilde{x}^{3k}$ that form the polynomial.

For a monomial inhomogeneity \tilde{x}^q with $q \in \mathbb{N}_0$, Eq. (30) reads

$$\partial_{\tilde{x}}^2 f - \tilde{x}\partial_{\tilde{x}} f - kf = \tilde{x}^q, \quad (\text{A1})$$

and by direct substitution it follows that a solution to this equation is

$$f(\tilde{x}) = -\frac{1}{k+q} \sum_{n=0}^{\lfloor q/2 \rfloor} \tilde{x}^{q-2n} \prod_{i=0}^{n-1} \frac{(q-2i)(q-1-2i)}{k+q-2(i+1)}, \quad (\text{A2})$$

with the floor function

$$\lfloor q/2 \rfloor = \begin{cases} q/2 & \text{if } q \text{ even,} \\ (q-1)/2 & \text{if } q \text{ odd.} \end{cases} \quad (\text{A3})$$

We see that the solution Eq. (A2) is a polynomial in \tilde{x} , and is of the same order as the monomial inhomogeneity on the right-hand side of Eq. (A1).

This finally implies that for the polynomial of order at most $3k$ on the right-hand side of Eq. (30), we have a solution \tilde{Q}_k that is a linear combination of terms of the form Eq. (A2), and as such is a polynomial in \tilde{x} of order at most $3k$, as claimed. We now show that this solution fulfills both the boundary and normalization condition.

First, for our polynomial solution $\tilde{Q}_k(\tilde{x})$ the product

$$\tilde{P}^{(k)}(\tilde{x}) \equiv \tilde{Q}_k(\tilde{x})\tilde{P}^{(0)}(\tilde{x}) \quad (\text{A4})$$

fulfills the boundary conditions Eq. (25), because a product of an exponential decay of $P^{(0)}$ with a finite polynomial eventually always decays. Our algorithm therefore leads to a term $\tilde{P}^{(k)}(\tilde{x})$ which solve the second-order ODE Eq. (A6) with the boundary conditions Eq. (25) at $\tilde{x} = \pm\infty$.

To show that the perturbative solution Eq. (22) conserves probability exactly, we rewrite the power series as

$$\tilde{P}(\tilde{x}, \tilde{t}) = \sum_{k=0}^{\infty} \tilde{\epsilon}^k(\tilde{t})\tilde{P}^{(k)}(\tilde{x}), \quad (\text{A5})$$

where $P^{(k)}$ is defined in Eq. (A4). Substituting Eqs. (A5), (26), (27) into Eq. (15), and demanding that the resulting equation hold at each order in $\tilde{\epsilon}$ separately, we obtain

$$\begin{aligned} \partial_{\tilde{x}}^2 \tilde{P}^{(k)} + \partial_{\tilde{x}} (\tilde{x}\tilde{P}^{(k)}) - k\tilde{P}^{(k)} \\ = \sum_{l=0}^{k-1} \tilde{A}_l \partial_{\tilde{x}} [\tilde{x}^l \tilde{P}^{(k-1-l)}] - \sum_{l=1}^k \tilde{D}_l \partial_{\tilde{x}}^2 [\tilde{x}^l \tilde{P}^{k-l}], \end{aligned} \quad (\text{A6})$$

where the sums on the right-hand side are defined as zero if the upper summation bound is smaller than the lower summation bound. Note that upon substituting Eq. (A4) into Eq. (A6) we recover Eq. (30).

By integrating Eq. (A6) over \tilde{x} from $-\infty$ to ∞ , and noting that from the form of Eq. (A4) with $\tilde{P}^{(0)}$ Gaussian and \tilde{Q}_k polynomial it follows that all terms involving spatial derivatives of $\tilde{P}^{(k)}$ vanish for $|\tilde{x}| \rightarrow \infty$, we see that for $k \geq 1$ it holds that

$$\int_{-\infty}^{\infty} d\tilde{x} \tilde{P}^{(k)}(\tilde{x}) = 0, \quad (\text{A7})$$

which implies

$$\int_{-\infty}^{\infty} d\tilde{x} \tilde{P}(\tilde{x}, \tilde{t}) = \sum_{k=0}^{\infty} \tilde{\epsilon}^k(\tilde{t}) \int_{-\infty}^{\infty} d\tilde{x} \tilde{P}^{(k)}(\tilde{x}) \quad (\text{A8})$$

$$= \int_{-\infty}^{\infty} d\tilde{x} \tilde{P}^{(0)}(\tilde{x}) = 1. \quad (\text{A9})$$

This shows that the perturbation series Eq. (22) conserves probability exactly at all orders.

2. Parity of the polynomials \tilde{Q}_k

We now show that the polynomial $\tilde{Q}_k(\tilde{x})$ is comprised of only even powers of \tilde{x} for k even (and $k = 0$) and only of odd powers of \tilde{x} for k odd. Phrased differently, we show that for all $k \in \mathbb{N}_0$ we have

$$\tilde{Q}_k(\tilde{x}) = (-1)^k \tilde{Q}_k(-\tilde{x}). \quad (\text{A10})$$

We proceed by induction in the order k . For $k = 0$ it follows from Eq. (33) that \tilde{Q}_0 fulfills Eq. (A10). For the induction step, we assume $k \geq 1$ and that all \tilde{Q}_l fulfill

Eq. (A10) for $l < k$. Then according to Eqs. (31), (32), the right-hand side of Eq. (30) is an even polynomial in \tilde{x} for k even, and an odd polynomial in \tilde{x} for k odd. From Eq. (A2) it then follows that also \tilde{Q}_k is an even (odd) polynomial for k even (odd).

We note that this in particular implies that for $n + k$ odd it holds that

$$\langle \tilde{x}^n \rangle^{(k)} \equiv \int_{-\infty}^{\infty} d\tilde{x} \tilde{x}^n \tilde{Q}_k(\tilde{x}) \tilde{P}^{(0)}(\tilde{x}) = 0, \quad (\text{A11})$$

since $\tilde{P}^{(0)}$ is an even function in \tilde{x} and the integral boundaries are symmetric around $\tilde{x} = 0$.

Appendix B: Second-order perturbative propagator in physical units

In Sect. IV of the main text we discuss both the normalization-preserving propagator (NPP) and the positivity-preserving propagator (PPP). In the present appendix we first give explicit expressions for both to second order in perturbation theory, i.e. to order $\tilde{\epsilon}^2 \sim \Delta t$. We then rewrite the PPP in terms of an arbitrary discretization scheme, from which we recover the usual pathwise medium entropy production using a midpoint discretization scheme. Finally, we validate the perturbative propagators from this appendix by comparison to an exact solution, similar to Sect. VI.

1. Normalization-preserving propagator

Using the definitions of the dimensionless units Eqs. (13-19), we can cast the NPP Eq. (36) back into physical units. To order $\tilde{\epsilon}^2 \sim \Delta t$ in perturbation theory, this yields

$$P(x, t | x_0, t_0) = \frac{1}{\sqrt{4\pi D(x_0)\Delta t}} \exp\left[-\frac{\Delta x^2}{4D(x_0)\Delta t}\right] \times \left[1 + \sqrt{\Delta t}Q^{(1/2)} + \Delta tQ^{(1)} + \mathcal{O}(\Delta t^{3/2})\right] \quad (\text{B1})$$

with $Q^{(k)} \equiv Q^{(k)}(\Delta x, \Delta t) \equiv \tilde{\epsilon}^k(\tilde{t})\tilde{Q}_k(\tilde{x})/\sqrt{\Delta t}^k$, so that

$$Q^{(1/2)} = \frac{\tilde{x}}{2\sqrt{D}} [2a - 3\partial_x D + \partial_x D \tilde{x}^2] \quad (\text{B2})$$

$$Q^{(1)} = 2 \left(\frac{a^2}{9D} + \frac{\partial_x a}{4} \right) (\tilde{x}^2 - 1) + \frac{a\partial_x D}{4D} (\tilde{x}^4 - 5\tilde{x}^2 + 2) + \frac{(\partial_x D)^2}{16D} (\tilde{x}^6 - 11\tilde{x}^4 + 21\tilde{x}^2 - 3) + \frac{\partial_x^2 D}{12} (2\tilde{x}^4 - 9\tilde{x}^2 + 3), \quad (\text{B3})$$

where D , a as well as their spatial derivatives are evaluated at x_0 , and where as before $\tilde{x} \equiv \Delta x/R \equiv \Delta x/\sqrt{2D(x_0)\Delta t}$.

2. Positivity-preserving propagator

To obtain the PPP Eq. (41) to order Δt in physical units, we substitute Eqs. (33), (34), (35) into Eq. (41), and substitute the definitions of our dimensionless units. This yields the short-time propagator

$$P(x, t | x_0, t_0) = \frac{1}{\sqrt{4\pi D(x_0)\Delta t}} \exp(-\Delta S) \quad (\text{B4})$$

with

$$\Delta S = \Delta S^{(0)} + \sqrt{\Delta t}\Delta S^{(1/2)} + \Delta t\Delta S^{(1)} + \mathcal{O}(\Delta t^{3/2}), \quad (\text{B5})$$

where

$$\Delta S^{(0)} = \frac{\Delta t}{4D} \left(\frac{\Delta x}{\Delta t} - a \right)^2, \quad (\text{B6})$$

$$\Delta S^{(1/2)} = \partial_x D \sqrt{\frac{2}{D}} \frac{\tilde{x}}{4} (3 - \tilde{x}^2) \quad (\text{B7})$$

$$\Delta S^{(1)} = \frac{\partial_x a}{2} (1 - \tilde{x}^2) + \frac{\partial_x^2 D}{12} (-2\tilde{x}^4 + 9\tilde{x}^2 - 3) + \frac{(\partial_x D)^2}{16D} (5\tilde{x}^4 - 12\tilde{x}^2 + 3) + \frac{a\partial_x D}{2D} (\tilde{x}^2 - 1)$$

where D , a and their spatial derivatives are all evaluated at x_0 , and where as before $\tilde{x} \equiv \Delta x/R \equiv \Delta x/\sqrt{2D(x_0)\Delta t}$. Recalling that the typical leading-order scaling of the increment is $\Delta x = \mathcal{O}(\Delta t^{1/2})$ in the range where Eq. (B4) is non-negligible, we note that $\Delta S^{(0)}$ contains terms of order Δt^0 , $\Delta t^{1/2}$, Δt^1 . On the other hand, all terms of $\Delta S^{(1/2)}$ scale to leading order as $\Delta t^{1/2}$ and all terms of $\Delta S^{(1)}$ scale to leading order as Δt .

For additive noise all terms that include $\partial_x D$, $\partial_x^2 D$ vanish, and Eq. (B5) reduces to the short-time propagator from Ref. [6], which is given by

$$\Delta S = \frac{\Delta t}{4D} \left(\frac{\Delta x}{\Delta t} - a \right)^2 - \frac{\partial_x a}{2D} (\Delta x^2 - 2D\Delta t) + \mathcal{O}(\Delta t^{3/2}). \quad (\text{B9})$$

The highest power in Δx which appears in this expression is Δx^2 , with a prefactor $1/(4D\Delta t) - \partial_x a/(2D)$. For small enough timestep Δt this prefactor is positive, so that in that case the resulting propagator Eq. (B4) fulfills the boundary conditions Eq. (20).

To discuss the boundary conditions for the general case of multiplicative noise, we note that the highest power in \tilde{x} that appears in Eq. (B5) is \tilde{x}^4 . According to Eq. (B8), the term with the highest power is given by $\Delta t \tilde{x}^4 / 2 [-\partial_x^2 D / 3 + 5\partial_x D / (8D)]$. If this factor has a negative sign, then the exponential in Eq. (B4) diverges as $|\tilde{x}| \rightarrow \infty$. Thus, the representation Eq. (B4) of the short-time propagator only fulfills the boundary conditions Eq. (20) if

$$\frac{15}{8} \frac{(\partial_x D)^2(x_0)}{D(x_0)} > (\partial_x^2 D)(x_0). \quad (\text{B10})$$

This condition is independent of the temporal breakdown condition Eq. (42). We mathematically associate Eq. (B10) with the finite radius of convergence $|z| = 1$ of the Taylor series Eq. (40) used in deriving the PPP; as $|\tilde{x}| \rightarrow \infty$, the corresponding values for $|z|$ are typically larger than 1. At this point we emphasize again that the short-time propagator should only be non-negligible for $|\tilde{x}| \lesssim 1$ due to the finite speed of diffusion; the breakdown of the boundary conditions in the PPP hence highlights the technical challenges for deriving approximate short-time solutions of the FP Eq. (1).

3. Midpoint discretization and path-wise entropy production

In all our results so far, a , D and all their derivatives are evaluated at the initial point x_0 , which corresponds to an initial point discretization scheme. To show how the propagator with respect to other discretization schemes is obtained from our results, we now rewrite the PPP Eq. (B4) with respect to an arbitrary discretization scheme, defined by a parameter $\alpha \in [0, 1]$. For this, we note that

$$x_0 = x_\alpha - \alpha\Delta x, \quad (\text{B11})$$

where $x_\alpha = x_0 + \alpha\Delta x$. While for $\alpha = 0$ we have $x_\alpha = x_0$ (initial point discretization scheme), for $\alpha = 1/2$ we have $x_\alpha = (x_0 + x)/2$ (midpoint discretization scheme). The value of any analytical function, $f(x_0)$, can be expressed via Taylor expansion around x_α as

$$f(x_0) = f(x_\alpha) - \alpha\Delta x (\partial_x f)(x_\alpha) + \frac{\alpha^2}{2} \Delta x^2 (\partial_x^2 f)(x_\alpha) + \mathcal{O}(\Delta x^3) \quad (\text{B12})$$

Substituting this Taylor expansion for $f \equiv a$, D , and their derivatives, into Eq. (B4), we obtain

$$P(x, t | x_0, t_0) = \frac{1}{\sqrt{4\pi D_\alpha \Delta t}} \exp(-\Delta S_\alpha) \quad (\text{B13})$$

where

$$\Delta S_\alpha = \Delta S_\alpha^{(0)} + \sqrt{\Delta t} \Delta S_\alpha^{(1/2)} + \Delta t \Delta S_\alpha^{(1)} + \mathcal{O}(\Delta t^{3/2}), \quad (\text{B14})$$

with the functions $\Delta \bar{S}^{(k)} \equiv \Delta \bar{S}^{(k)}(\Delta x, \Delta t, \bar{X})$ are given by

$$\Delta S_\alpha^{(0)} = \frac{\Delta t}{4D_\alpha} \left(\frac{\Delta x}{\Delta t} - a_\alpha + 2\alpha \partial_x D_\alpha \right)^2, \quad (\text{B15})$$

$$\Delta S_\alpha^{(1/2)} = \partial_x D_\alpha \sqrt{\frac{2}{D_\alpha}} \frac{\tilde{x}_\alpha}{4} (2\alpha - 1) (\tilde{x}_\alpha^2 - 3) \quad (\text{B16})$$

$$\begin{aligned} \Delta S_\alpha^{(1)} = & \frac{\partial_x a_\alpha}{2} (2\alpha \tilde{x}_\alpha^2 - \tilde{x}_\alpha^2 + 1) \\ & + \frac{\partial_x^2 D_\alpha}{12} (-6\alpha^2 \tilde{x}_\alpha^2 (\tilde{x}_\alpha^2 - 1) \\ & \quad + 6\alpha \tilde{x}_\alpha^2 (\tilde{x}_\alpha^2 - 3) - 2\tilde{x}_\alpha^4 + 9\tilde{x}_\alpha^2 - 3) \\ & + \frac{a_\alpha \partial_x D_\alpha}{2D_\alpha} (\tilde{x}_\alpha^2 - 1) (1 - 2\alpha) \quad (\text{B17}) \\ & + \frac{(\partial_x D_\alpha)^2}{16D_\alpha} (16\alpha^2 \tilde{x}_\alpha^4 - 8\alpha^2 \tilde{x}_\alpha^2 - 16\alpha^2 - 16\alpha \tilde{x}_\alpha^4 \\ & \quad + 24\alpha \tilde{x}_\alpha^2 + 5\tilde{x}_\alpha^4 - 12\tilde{x}_\alpha^2 + 3). \end{aligned}$$

Here, $\tilde{x}_\alpha \equiv \Delta x / \sqrt{2D_\alpha \Delta t}$.

For the midpoint convention, $\alpha = 1/2$, we write

$$\tilde{x}_{\alpha=1/2} \equiv \bar{x} \equiv \frac{x_0 + x}{2}, \quad (\text{B18})$$

and it holds that $\Delta S_\alpha^{(1/2)} = 0$. We therefore write Eq. (B14) as

$$\Delta \bar{S} = \Delta \bar{S}^{(0)} + \Delta t \Delta \bar{S}^{(1)} + \mathcal{O}(\Delta t^{3/2}), \quad (\text{B19})$$

with the functions $\Delta \bar{S}^{(k)} \equiv \Delta \bar{S}^{(k)}(\Delta x, \Delta t, \bar{X})$ from Eqs. (B15), (B17) reducing to

$$\Delta \bar{S}^{(0)} = \frac{\Delta t}{4\bar{D}} \left(\frac{\Delta x}{\Delta t} - \bar{a} + \partial_x \bar{D} \right)^2, \quad (\text{B20})$$

$$\begin{aligned} \Delta \bar{S}^{(1)} = & \frac{1}{2} \partial_x \bar{a} + \frac{\partial_x^2 \bar{D}}{24} (-\bar{x}^4 + 3\bar{x}^2 - 6) \\ & + \frac{(\partial_x \bar{D})^2}{16\bar{D}} (\bar{x}^4 - 2\bar{x}^2 - 1). \quad (\text{B21}) \end{aligned}$$

We here use a bar to denote that the expression is evaluated at \bar{x} , e.g. $\bar{a} \equiv a(\bar{x})$, $\partial_x \bar{D} \equiv (\partial_x D)(\bar{x})$, and where $\bar{x} \equiv \Delta x / \sqrt{2\bar{D}\Delta t}$. We remark that despite the lack of an explicit term $\Delta \bar{S}^{(1/2)}$ in Eq. (B19), the contribution Eq. (B20) contains terms of order $\Delta x \sim \sqrt{\Delta t}$.

As for the PPP with initial-point evaluation, Eq. (B4), there is no a-priori guarantee that the midpoint-evaluated propagator with Eq. (B19) decays to zero as $|\Delta x| \rightarrow \infty$. The leading order term in Δx is given by the quartic powers in Eq. (B21), so that for large $|\Delta x|/L$ we have

$$\Delta \bar{S} \approx \frac{\Delta t \bar{x}^4}{8} \left(-\frac{\partial_x^2 \bar{D}}{3} + \frac{(\partial_x \bar{D})^2}{2} \right). \quad (\text{B22})$$

In the midpoint evaluation scheme both $\partial_x^2 \bar{D}$ and $\partial_x \bar{D}$ depend on Δx , because they are always evaluated at the

midpoint $x_0 + \Delta x/2$. Thus, depending on the details of the diffusivity profile, as $|\Delta x|/L \rightarrow \infty$ the sign of Eq. (B22) can be either positive or negative, or even oscillate.

The short-time propagator in the midpoint evaluation scheme is the usual starting point for deriving the path-wise entropy production [13, 33, 34], and we now show that the propagator Eq. (B13) with $\alpha = 1/2$ leads to the usual result.

For this, we consider a path $\varphi(t)$ with $t \in [0, t_f]$. We discretize the time interval $[0, t_f]$ into N equal subintervals $[t_i, t_{i+1}]$ with $t_i \equiv t_f \cdot i/N$. The discretized probability density for the path φ is then defined as

$$P_N[\varphi] \equiv \prod_{i=0}^{N-1} P(\varphi_{i+1}, t_{i+1} | \varphi_i, t_i), \quad (\text{B23})$$

where $\varphi_i \equiv \varphi(t_i)$. The medium entropy production $\Delta s_m[\varphi]$ of the path φ is then obtained as the negative log-ratio of the $N \rightarrow \infty$ limit for the probability density ratio of a pair of forward- and backward path, with the latter defined as $\varphi^b(t) \equiv \varphi(t_f - t)$ [13, 33, 34]. Substituting Eq. (B23) for the forward and backward path pair and using the midpoint-discretized propagator [13, 60], we obtain

$$\Delta s_m[\varphi] \equiv - \lim_{N \rightarrow \infty} \ln \frac{P[\varphi]}{P[\varphi^b]} \quad (\text{B24})$$

$$= - \lim_{N \rightarrow \infty} \prod_{i=0}^{N-1} \ln \frac{P(\varphi_{i+1}, t_{i+1} | \varphi_i, t_i)}{P(\varphi_i, t_{i+1} | \varphi_{i+1}, t_i)} \quad (\text{B25})$$

$$= - \lim_{N \rightarrow \infty} \sum_{i=0}^{N-1} [\Delta \bar{S}(\Delta \varphi_i, \Delta t, \bar{\varphi}_i) - \Delta \bar{S}(-\Delta \varphi_i, \Delta t, \bar{\varphi}_i)], \quad (\text{B26})$$

where $\Delta \varphi_i \equiv \varphi_{i+1} - \varphi_i$, $\bar{\varphi}_i \equiv (\varphi_{i+1} + \varphi_i)/2$. From Eq. (B26) it is apparent that only those terms from $\Delta \bar{S}(\Delta \varphi_i, \Delta t, \bar{\varphi}_i)$ contribute that are odd under the reflection $\Delta \varphi_i \rightarrow -\Delta \varphi_i$. These are precisely the terms in Eq. (B19) that are linear in Δx , which are all contained in Eq. (B20). In particular, all terms of order Δt from Eq. (B21) are even under the reflection $\Delta x \rightarrow -\Delta x$, and are hence not relevant for the medium entropy production. Therefore, the propagator to order $\sqrt{\Delta t} \sim \Delta x$ in the exponent, which includes the GP, is in fact sufficient to derive the path-wise entropy production.

After substituting the explicit expression for $\Delta \bar{S}$, we obtain the continuum limit

$$\Delta s_m[\varphi] = \int_0^T dt \dot{\varphi}(t) \frac{a(\varphi(t)) - (\partial_x D)(\varphi(t))}{D(\varphi(t))}, \quad (\text{B27})$$

which is the usual formula for the entropy production for a multiplicative-noise system [35, 61].

4. Comparison of quadratic-order propagators to exact solution

In Sect. VI of the main text we compare our perturbative results to an explicit example system. In the present appendix we extend the comparison to the quadratic-order propagators from the previous subsections, namely the NPP Eq. (B1), the PPP with initial-point evaluation Eq. (B4), and the PPP with midpoint evaluation, Eq. (B13) with $\alpha = 1/2$.

In Fig. 5 (a), (b) we plot both the exact solution (black solid line) and the perturbative propagators (broken colored lines) for (a) $\Delta t/T = 0.05$ and (b) $\Delta t/T = 0.2$. In Fig. 5 (a) we observe that for $\Delta t/T = 0.05$, all perturbative solutions agree very well with the exact solution on the plotting scales. We confirm this in Fig. 5 (d), where we show that the instantaneous error Eq. (44) for all approximations is small compared to the typical function values of the probability densities. The plot also shows that while the error for all approximate propagators is of the same order, the NPP with $K = 2$ and midpoint evaluation rule leads to a slightly smaller error.

In Fig. 5 (b) we consider the time increment $\Delta t/T = 0.2$. While the PPP with $K = 2$ and midpoint evaluation scheme still agrees very well with the exact solution, the other two propagators deviate visibly from the exact solution for $x/L \approx \pm 2$. This is also clearly seen in Fig. 5 (e), where we show the pointwise error for $\Delta t/T = 0.2$.

In Fig. 5 (c) we show the L^1 -error Eq. (43) as a function of Δt for all approximate solutions. While the errors in the NPP and PPP with initial-point evaluation are almost identical in magnitude, for $\Delta t \ll \Delta t_b$ these errors are approximately a factor of five larger as compared to the error in the PPP with midpoint evaluation. As the running exponents Eq. (5) in Fig. 5 (f) show, for all approximate propagators the error scales as $E \sim \Delta t^{3/2}$ for $\Delta t \ll \Delta t_b$; this is in agreement with our estimate Eq. (46).

While the PPPs we consider here decay to zero at the bounds of the domain we consider here, we again emphasize that this is not self-evident. For the diffusivity and drift shown in Fig. 5 and the initial value $x_0/L = 0.5$ we have $15(\partial_x D)^2(x_0)/(8D(x_0))T \approx 0.35 > -0.29 \approx (\partial_x^2 D)(x_0)T$, so that according to Eq. (B10) the PPP fulfills the boundary conditions Eq. (20). On the other hand, for example for $x_0/L = 1$ it holds that $15(\partial_x D)^2(x_0)/(8D(x_0))T \approx 0.04 < 1.44 \approx (\partial_x^2 D)(x_0)T$, so that the representation Eq. (B4) diverges as $|\Delta x/L| \rightarrow \infty$.

Appendix C: Moments in physical units

In Sect. V, we discuss the perturbative calculation of the moments $\langle \Delta x^n \rangle$. In physical units, Eq. (48) yields a

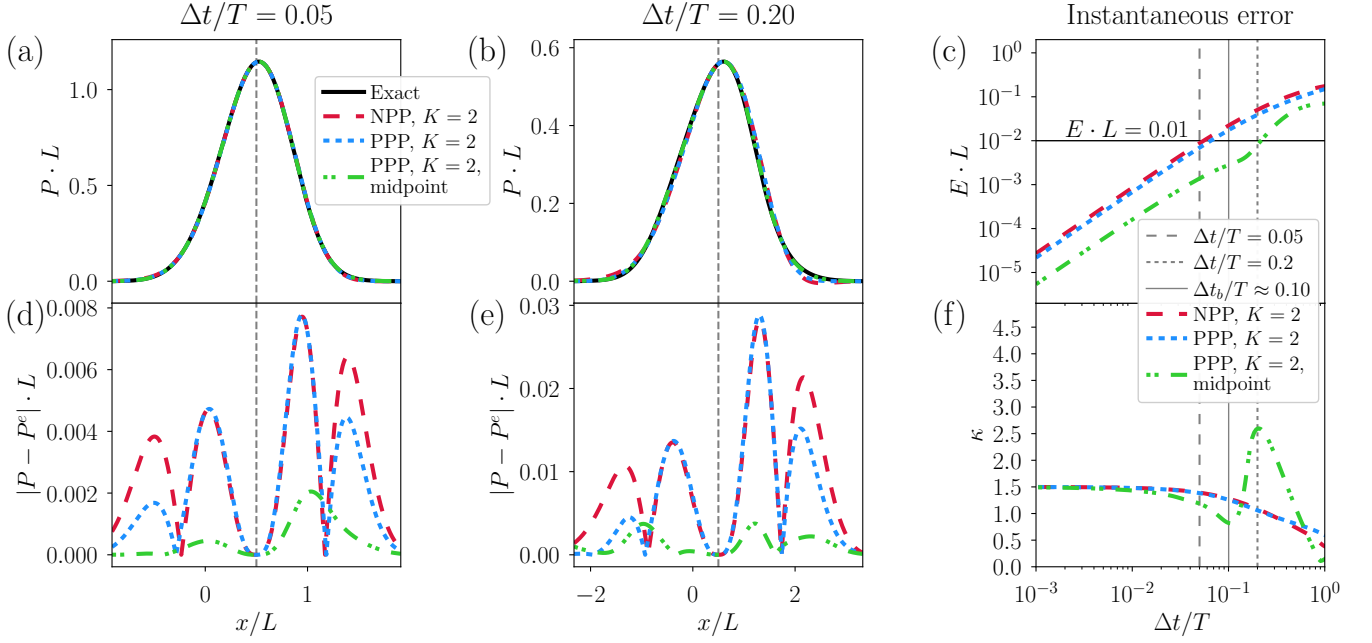


Figure 5. **Comparison of normalization-preserving propagator (NPP), positivity-preserving propagator (PPP), and PPP using a midpoint-evaluation convention.** Throughout this figure, we plot data pertaining to the normalization-preserving propagator (NPP) for $K = 2$, Eq. (B1), as blue dotted lines. We furthermore show data based on the positivity-preserving propagator (PPP) for $K = 2$, Eq. (B4) for $K = 2$ as red dashed lines, and data obtained using the PPP for $K = 2$ with midpoint evaluation, Eq. (B13) with $\alpha = 1/2$, as green dash-dotted lines. For all data we use the drift and diffusivity from Fig. 1, as well as the initial condition $x_0/L = 0.5$. In subplots (a), (b) we plot the exact solution P^e (black solid line), together with various approximate propagators; we show the respective pointwise error Eq. (44) in subplots (d) and (e). While subplots (a), (d) correspond to a lagtime $\Delta t/T = 0.05$, for (b), (e) we use $\Delta t/T = 0.2$. The legend in subplot (a) is valid for subplots (a), (b), (d), (e). In subplot (c) we show the L^1 error Eq. (43) for all approximate propagators considered; in subplot (f) we plot the corresponding local exponent Eq. (71). The vertical broken lines in subplots (c), (f) denote the lagtimes used for subplots (a), (b), (d), (e), the vertical solid line indicates the breakdown time $\Delta t_b/T \approx 0.10$ as defined in Eq. (42). The horizontal solid line in subplot (c) indicates the error $E_p \cdot L = 0.01 = 1\%$.

perturbation expansion

$$\langle \Delta x^n \rangle = \sum_{k=0}^{\infty} \Delta t^k \langle \Delta x^n \rangle^{(k)}. \quad (\text{C1})$$

Using Eq. (49), we find that for $n = 0$, we have $\langle \Delta x^0 \rangle^{(k)} = \delta_{k,0}$. In the following, we furthermore give the lowest-order terms of Eq. (C1) for $n = 1, 2, 3$. In all the expressions, a , D , and their derivatives are evaluated at x_0 .

$n = 1$:

$$\langle \Delta x \rangle^{(0)} = 0, \quad (\text{C2})$$

$$\langle \Delta x \rangle^{(1)} = a, \quad (\text{C3})$$

$$2\langle \Delta x \rangle^{(2)} = Da^{(2)} + aa^{(1)}, \quad (\text{C4})$$

$$\begin{aligned} 6\langle \Delta x \rangle^{(3)} = & a(a^{(1)})^2 + a^2a^{(2)} + D^2a^{(4)} \\ & + 3Da^{(1)}a^{(2)} + 2DD^{(1)}a^{(3)} + 2Daa^{(3)} \\ & + DD^{(2)}a^{(2)} + D^{(1)}aa^{(2)}, \end{aligned} \quad (\text{C5})$$

$n = 2$:

$$\langle \Delta x^2 \rangle^{(0)} = 0, \quad (\text{C6})$$

$$\langle \Delta x^2 \rangle^{(1)} = 2D, \quad (\text{C7})$$

$$\langle \Delta x^2 \rangle^{(2)} = a^2 + DD^{(2)} + D^{(1)}a + 2Da^{(1)}, \quad (\text{C8})$$

$$\begin{aligned} 3\langle \Delta x^2 \rangle^{(3)} = & 3a^2a^{(1)} + D(D^{(2)})^2 + D^{(2)}a^2 \\ & + D^2D^{(4)} + 4D(a^{(1)})^2 + 4D^2a^{(3)} \\ & + 3D^{(1)}aa^{(1)} + D^{(1)}D^{(2)}a + 2DD^{(1)}D^{(3)} \\ & + 2DD^{(3)}a + 4DD^{(2)}a^{(1)} + 7DD^{(1)}a^{(2)} \\ & + 7Daa^{(2)}, \end{aligned} \quad (\text{C9})$$

$n = 3$:

$$\langle \Delta x^3 \rangle^{(0)} = 0, \quad (\text{C10})$$

$$\langle \Delta x^3 \rangle^{(1)} = 0, \quad (\text{C11})$$

$$\langle \Delta x^3 \rangle^{(2)} = 6DD^{(1)} + 6Da, \quad (\text{C12})$$

$$\begin{aligned} \langle \Delta x^3 \rangle^{(3)} = & a^3 + 2(D^{(1)})^2a + 3D^{(1)}a^2 \\ & + 4D^2D^{(3)} + 7D^2a^{(2)} + 7DD^{(2)}a \\ & + 8DD^{(1)}D^{(2)} + 9Daa^{(1)} + 10DD^{(1)}a^{(1)}. \end{aligned} \quad (\text{C13})$$

These expressions, as well as higher order terms up to $\langle \Delta x^n \rangle^{(k)}$ for $n = 0, 1, 2, 3, 4$ and $k = 0, 1, \dots, 4$, are given as symbolic expressions in the python module PySTFP [45].

Appendix D: Perturbative entropy production

Following the stochastic thermodynamics literature [13, 34] we define the non-equilibrium Gibbs entropy

$$S(t) \equiv - \int_{-\infty}^{\infty} dx P(x, t) \ln [P(x, t)L], \quad (\text{D1})$$

where here $P(x, t) \equiv P(x, t | x_0, t_0)$, and where in the logarithm we multiply P by the length scale L in order to render the argument of the logarithm dimensionless. By taking the time derivative of this entropy, and using the FP Eq. (1), we obtain [13, 34]

$$\dot{S}(t) = \dot{S}^{\text{tot}}(t) - \dot{S}^{\text{m}}(t), \quad (\text{D2})$$

with the total- and medium entropy production

$$\dot{S}^{\text{tot}}(t) \equiv \int_{-\infty}^{\infty} dx \frac{j(x, t)^2}{D(x)P(x, t)}, \quad (\text{D3})$$

$$\dot{S}^{\text{m}}(t) \equiv \int_{-\infty}^{\infty} dx \frac{j(x, t)}{D(x)} [a(x) - (\partial_x D)(x)], \quad (\text{D4})$$

with the standard FP probability flux

$$j \equiv aP - \partial_x(DP). \quad (\text{D5})$$

To evaluate Eqs. (D1), (D3), (D4) perturbatively, we first rewrite the expressions in dimensionless form using Eqs. (16-19). This yields

$$\tilde{S}(\tilde{t}) \equiv S(t) = - \int_{-\infty}^{\infty} d\tilde{x} \tilde{P}(\tilde{x}, \tilde{t}) \ln \left[\frac{\tilde{P}(\tilde{x}, \tilde{t})}{\tilde{\epsilon}(\tilde{t})} \right], \quad (\text{D6})$$

$$\dot{\tilde{S}}^{\text{tot}}(\tilde{t}) \equiv \tau_D \dot{S}^{\text{tot}}(t) = \tilde{\epsilon}^2 \int_{-\infty}^{\infty} d\tilde{x} \frac{\tilde{j}(\tilde{x}, \tilde{t})^2}{\tilde{D}(\tilde{x}, \tilde{t})\tilde{P}(\tilde{x}, \tilde{t})}, \quad (\text{D7})$$

$$\dot{\tilde{S}}^{\text{m}}(\tilde{t}) \equiv \tau_D \dot{S}^{\text{m}}(t) = \int_{-\infty}^{\infty} d\tilde{x} \frac{\tilde{j}(\tilde{x}, \tilde{t})}{\tilde{D}(\tilde{x}, \tilde{t})} \left[\tilde{\epsilon}\tilde{a} - (\partial_{\tilde{x}}\tilde{D}) \right], \quad (\text{D8})$$

with the dimensionless probability flux

$$\tilde{j} \equiv \tau_D j \equiv \frac{1}{\tilde{\epsilon}^2} \left[\tilde{\epsilon}\tilde{a}\tilde{P} - \partial_{\tilde{x}}(\tilde{D}\tilde{P}) \right]. \quad (\text{D9})$$

We now discuss the perturbative evaluation of Eqs. (D6), (D7), (D8).

First, to evaluate Eq. (D6) perturbatively, we substitute the power series expansion Eq. (23) for \tilde{P} into the logarithm and use the standard rules for manipulating

logarithms, as well as the normalization of the perturbative propagator, to derive

$$\begin{aligned} \tilde{S}(\tilde{t}) &= \frac{1}{2} \ln(2\pi\tilde{\epsilon}^2) + \frac{1}{2} \int_{-\infty}^{\infty} d\tilde{x} \tilde{P}(\tilde{x}, \tilde{t}) \tilde{x}^2 \\ &\quad - \int_{-\infty}^{\infty} d\tilde{x} \tilde{P}(\tilde{x}, \tilde{t}) \ln \left[1 + \sum_{k=1}^{\infty} \tilde{\epsilon}(\tilde{t})^k \tilde{Q}_k(\tilde{x}, \tilde{t}) \right]. \end{aligned} \quad (\text{D10})$$

Upon expanding the logarithm in the second line in powers of $\tilde{\epsilon}$, and substituting Eq. (23) into the integrands, both integrands in Eq. (D10) become sums over terms that are each a product of a polynomial in \tilde{x} with a Gaussian. These integrals are easily evaluated, so that to leading order we obtain

$$\begin{aligned} \tilde{S} &= \frac{1}{2} [1 + \ln(2\pi\tilde{\epsilon}^2)] \\ &\quad + \frac{\tilde{\epsilon}^2}{16} [2\mathcal{A}_0\mathcal{D}_1 + 4\mathcal{A}_1 - 3\mathcal{D}_1^2 + 4\mathcal{D}_2] + \mathcal{O}(\tilde{\epsilon}^4). \end{aligned} \quad (\text{D11})$$

In the python module PySTFP [45] we provide the power series coefficients up to order $\tilde{\epsilon}^8 \sim \Delta t^4$ in symbolic form.

We now evaluate the medium entropy production rate Eq. (D8) perturbatively. For this we first use integration by parts to rewrite the integral as

$$\begin{aligned} \dot{\tilde{S}}^{\text{m}}(\tilde{t}) &= \int_{-\infty}^{\infty} d\tilde{x} \tilde{P}(\tilde{x}, \tilde{t}) \\ &\quad \times \left[\frac{1}{\tilde{D}} \left(\tilde{a} - \frac{1}{\tilde{\epsilon}} \partial_{\tilde{x}} \tilde{D} \right)^2 + \frac{1}{\tilde{\epsilon}} \partial_{\tilde{x}} \left(\tilde{a} - \frac{1}{\tilde{\epsilon}} \partial_{\tilde{x}} \tilde{D} \right) \right], \end{aligned} \quad (\text{D12})$$

where in our notation we suppress the arguments of $\tilde{a}(\tilde{x}, \tilde{t})$, $\tilde{D}(\tilde{x}, \tilde{t})$, $\tilde{\epsilon}(\tilde{t})$. Equation (D12) has the form of an expectation value integral, and by substituting the perturbation series Eq. (23), (26), (27) in the integral, we evaluate it perturbatively to any desired order. We note that despite the explicit appearance of a factor $1/\tilde{\epsilon}^2$ in Eq. (D12), the leading order is actually $\tilde{\epsilon}^0$. This follows by substituting the perturbation series for \tilde{a} , \tilde{D} , and evaluating the spatial derivatives that appear in the second factor in Eq. (D12); consequently, we conclude that $\dot{\tilde{S}}^{\text{m}} = \mathcal{O}(\tilde{\epsilon}^0)$. More explicitly, to leading order in $\tilde{\epsilon}$ we obtain

$$\dot{\tilde{S}}^{\text{m}} = (\mathcal{A}_0 - \mathcal{D}_1)^2 + \mathcal{A}_1 - 2\mathcal{D}_2 + \mathcal{O}(\tilde{\epsilon}^2). \quad (\text{D13})$$

In the python module PySTFP [45] we provide the power series coefficients up to order $\tilde{\epsilon}^8 \sim \Delta t^4$ in symbolic form.

By contrast, since the integrand in the total entropy production rate Eq. (D7) is quadratic in \tilde{P} , the expression cannot be rewritten in the form of an expectation value of a \tilde{P} -independent function. We can evaluate the integral nonetheless perturbatively, by substituting the power series expansions of \tilde{P} , \tilde{a} , \tilde{D} , sorting the resulting integrand by powers of $\tilde{\epsilon}$, and evaluating the integrals (which are products of polynomials and a Gaussian) up

to the desired order. The resulting leading order contributions are

$$\dot{S}^{\text{tot}} = \frac{1}{\tilde{\epsilon}^2} + \frac{1}{8} \left(8\tilde{\mathcal{A}}_0 - 14\tilde{\mathcal{A}}_0\tilde{\mathcal{D}}_1 + 12\tilde{\mathcal{A}}_1 + 5\tilde{\mathcal{D}}_1^2 - 12\tilde{\mathcal{D}}_2 \right) + \mathcal{O}(\tilde{\epsilon}^2). \quad (\text{D14})$$

In the python module PySTFP [45] we provide the power series coefficients up to order $\tilde{\epsilon}^6 \sim \Delta t^3$ in symbolic form.

Recasting the power series Eqs. (D11), (D13), (D14) in physical dimensions we then obtain

$$S = \frac{1}{2} \left[1 + \ln \left(\frac{4\pi D \Delta t}{L^2} \right) \right] + \frac{\Delta t}{8D} [2a\partial_x D + 4(\partial_x a)D + 2(\partial_x^2 D)D - 3(\partial_x D)^2] + \mathcal{O}(\Delta t^2), \quad (\text{D15})$$

$$\dot{S}^{\text{m}} = \frac{1}{D} (a - \partial_x D)^2 + \partial_x a - \partial_x^2 D + \mathcal{O}(\Delta t), \quad (\text{D16})$$

$$\dot{S}^{\text{tot}} = \frac{1}{2\Delta t} + \frac{1}{8D} [8a^2 - 14a\partial_x D + 12(\partial_x a)D - 6D\partial_x^2 D + 5(\partial_x D)^2] + \mathcal{O}(\Delta t), \quad (\text{D17})$$

where a , D , and their derivatives are evaluated at the initial position x_0 . We note that Eq. (D15) explicitly depends on L , which is because in Eq. (D1) we include a factor L to render the argument of the logarithm dimensionless.

Appendix E: Medium entropy production as rate of change of potential energy

We now discuss how Eq. (D4) can be reformulated in terms of a potential energy for systems where the latter is defined [56, 57].

We consider a system where a zero-flux steady state P_{steady} exists, which by definition fulfils

$$\partial_x (D P_{\text{steady}}) - a P_{\text{steady}} = 0 \quad (\text{E1})$$

everywhere. Integrating this equation it follows that

$$P_{\text{steady}}(x) = \frac{\mathcal{N}(x_{\text{ref}})}{D(x)} \exp \left[\int_{x_{\text{ref}}}^x dx' \frac{a(x')}{D(x')} \right] \quad (\text{E2})$$

where x_{ref} is arbitrary and $\mathcal{N}(x_{\text{ref}})$ is a normalization constant so that P_{steady} is a properly normalized probability density.

Via Boltzmann inversion, we obtain the corresponding potential $U(x)$ as

$$U(x) = -\ln [P_{\text{steady}}(x)L] \quad (\text{E3})$$

$$= \ln \left[\frac{D(x)}{D_0} \right] - \int_{x_{\text{ref}}}^x dx' \frac{a(x')}{D(x')} + U_0, \quad (\text{E4})$$

where $U_0 = -\ln[LN(x_{\text{ref}})/D_0]$ is independent of x . Note that our definition of U makes the potential a dimensionless quantity, which one can think of as the potential

being expressed in units of the thermal energy (what we write U here is sometimes denoted as βU).

Taking the derivative of Eq. (E4) with respect to x , we obtain

$$\partial_x U = -\frac{1}{D(x)} [a(x) - (\partial_x D)(x)] \quad (\text{E5})$$

We therefore have

$$\dot{S}^{\text{m}}(t) \equiv \int_{-\infty}^{\infty} dx \frac{j(x,t)}{D(x)} [a(x) - (\partial_x D)(x)] \quad (\text{E6})$$

$$= -\int_{-\infty}^{\infty} dx j(x,t) (\partial_x U)(x) \quad (\text{E7})$$

$$= \int_{-\infty}^{\infty} dx (\partial_x j)(x,t) (U)(x) \quad (\text{E8})$$

$$= -\int_{-\infty}^{\infty} dx (\partial_t P)(x,t) U(x) \quad (\text{E9})$$

$$= -\partial_t \langle U \rangle, \quad (\text{E10})$$

where at Eq. (E7) we use integration by parts (and that vanishing-flux boundary conditions at $x = \pm\infty$ for j), at Eq. (E9) we use the FP Eq. (1) and at Eq. (E10) we use that U is time-independent.

Appendix F: Analytical solution for multiplicative-noise example system

For our numerical examples, we now construct a non-trivial one-dimensional multiplicative-noise system with a known analytical solution. For that we first consider the free-diffusion Fokker-Planck equation

$$\partial_t P_Y = D_0 \partial_y^2 P_Y \quad (\text{F1})$$

in a coordinate system (y,t) , and with a constant diffusivity D_0 . With delta-peak initial condition at y_0 , and vanishing boundary conditions at $|y| \rightarrow \infty$, Eq. (F1) is solved by

$$P_Y(y,t | y_0, t_0) = \frac{1}{\sqrt{4\pi D_0 \Delta t}} \exp \left[-\frac{(y - y_0)^2}{4D_0 \Delta t} \right], \quad (\text{F2})$$

where $\Delta t = t - t_0$.

We define a coordinate transformation $x \equiv \Phi(y)$, and rewrite the Fokker-Planck Eq. (F1) with respect to the new coordinate x . This leads to [1]

$$\partial_t P = -\partial_x (aP) + \partial_x^2 (DP), \quad (\text{F3})$$

where

$$a(x) = D_0 (\partial_y^2 \Phi) \Big|_{y=\Phi^{-1}(x)}, \quad (\text{F4})$$

$$D(x) = D_0 \left[(\partial_y \Phi) \Big|_{y=\Phi^{-1}(x)} \right]^2. \quad (\text{F5})$$

The solution to Eq. (F3), (F4), (F5) with delta-peak initial condition at x_0 is then given by

$$P(x, t | x_0, t_0) = \left[\left(\frac{d\Phi}{dy} \right)^{-1} P_Y(y, t | y_0, t_0) \right] \Big|_{y=\Phi^{-1}(x)}, \quad (\text{F6})$$

where $y_0 = \Phi^{-1}(x_0)$ and P_Y is given by Eq. (F2).

For the explicit example system considered in the main text we introduce a length scale L and a time scale T , and set $D_0 = L^2/T$. As coordinate transformation we use

$$\Phi(y) \equiv 0.35\pi y + 0.025L \sin\left(\pi \frac{y}{L}\right), \quad (\text{F7})$$

so that it follows from Eqs. (F4), (F5), that

$$a(x) = -\frac{L}{T} 0.025\pi^2 \sin\left(\pi \frac{\Phi^{-1}(x)}{L}\right), \quad (\text{F8})$$

$$D(x) = \frac{L^2}{T} \pi \left[0.35 + 0.025 \cos\left(\pi \frac{\Phi^{-1}(x)}{L}\right) \right]^2, \quad (\text{F9})$$

$$P(x, t | x_0, t_0) = \frac{1}{\pi} \left[0.35 + 0.025 \cos\left(\pi \frac{\Phi^{-1}(x)}{L}\right) \right]^{-1} \times \frac{1}{\sqrt{4\pi D_0 \Delta t}} \exp \left[-\frac{(\Phi^{-1}(x) - \Phi^{-1}(x_0))^2}{4D_0 \Delta t} \right] \quad (\text{F10})$$

To evaluate $\Phi^{-1}(x)$ numerically we use that for any x , finding y such that $y = \Phi^{-1}(x)$ is equivalent to finding the root of the function $g(y) \equiv \Phi(y) - x$. To do this in our numerical implementation we use the function `root_scalar` from `scipy.optimize` [62].

For our perturbative solution we need to calculate the derivatives of a , D , P , at x_0 . For this, we note that Eqs. (F4), (F5), (F6) are all of the form

$$f(x) = g(\Phi^{-1}(x)), \quad (\text{F11})$$

for explicitly given g . For example, for Eq. (F5) we have $f = D$ and $g = D_0(\partial_y \Phi)^2$. We furthermore note that from Eq. (F7), we can straightforwardly evaluate the derivatives of Φ with respect to y . We thus seek a formula for the derivatives of f , in terms of the derivatives of g and Φ . To obtain such a formula, we note that Eq. (F11) is equivalent to

$$f(\Phi(y)) = g(y). \quad (\text{F12})$$

By taking n derivatives of this equation with respect to y , we obtain an analytical formula for $(\partial_x^n f)(\Phi(y))$ with the need to know the explicit form of Φ^{-1} . We then evaluate the derivative at x_0 by substituting y with a numerically calculated $y_0 \equiv \Phi^{-1}(x_0)$. We use this procedure to calculate all analytical derivatives for a , D , P . The code for all evaluations of the analytical solution, and the derivatives of drift, diffusivity, and transition density, are provided in the python module `PySTFP` [45].

-
- [1] Hannes Risken, *The Fokker-Planck Equation: Methods of Solution and Applications* (Springer Berlin Heidelberg, Berlin, Heidelberg, 1996) oCLC: 906698554.
- [2] Nico G. van Kampen, *Stochastic processes in physics and chemistry*, 3rd ed., North-Holland personal library (Elsevier, Amsterdam ; Boston, 2007) oCLC: ocm81453662.
- [3] Crispin W. Gardiner, *Stochastic methods: a handbook for the natural and social sciences*, 4th ed., Springer series in synergetics (Springer, Berlin, 2009).
- [4] Paul C. Bressloff, *Stochastic Processes in Cell Biology*, Interdisciplinary Applied Mathematics, Vol. 41 (Springer International Publishing, Cham, 2014).
- [5] J. Gladrow, M. Ribezzi-Crivellari, F. Ritort, and U. F. Keyser, “Experimental evidence of symmetry breaking of transition-path times,” *Nature Communications* **10**, 55 (2019).
- [6] Jannes Gladrow, Ulrich F. Keyser, R. Adhikari, and Julian Kappler, “Experimental Measurement of Relative Path Probabilities and Stochastic Actions,” *Physical Review X* **11**, 031022 (2021).
- [7] Alice L. Thorneywork, Jannes Gladrow, Ulrich F. Keyser, Michael E. Cates, Ronjojoy Adhikari, and Julian Kappler, “Resolution dependence of most probable pathways with state-dependent diffusivity,” (2024), arXiv:2402.01559 [cond-mat, physics:physics].
- [8] H. Haken, “Generalized Onsager-Machlup function and classes of path integral solutions of the Fokker-Planck equation and the master equation,” *Zeitschrift für Physik B Condensed Matter and Quanta* **24**, 321–326 (1976).
- [9] Robert Graham, “Path integral formulation of general diffusion processes,” *Zeitschrift für Physik B Condensed Matter and Quanta* **26**, 281–290 (1977).
- [10] Katharine L. C. Hunt and John Ross, “Path integral solutions of stochastic equations for nonlinear irreversible processes: The uniqueness of the thermodynamic Lagrangian,” *The Journal of Chemical Physics* **75**, 976–984 (1981).
- [11] Artur B. Adib, “Stochastic Actions for Diffusive Dynamics: Reweighting, Sampling, and Minimization,” *The Journal of Physical Chemistry B* **112**, 5910–5916 (2008).
- [12] Peter Arnold, “Langevin equations with multiplicative noise: Resolution of time discretization ambiguities for equilibrium systems,” *Physical Review E* **61**, 6091–6098 (2000).
- [13] Udo Seifert, “Stochastic thermodynamics, fluctuation theorems, and molecular machines,” *Reports on Progress in Physics* **75**, 126001 (2012), arXiv: 1205.4176.
- [14] Ying Tang, Ruoshi Yuan, and Ping Ao, “Summing over trajectories of stochastic dynamics with multiplicative noise,” *The Journal of Chemical Physics* **141**, 044125 (2014).
- [15] Carson C. Chow and Michael A. Buice, “Path Integral Methods for Stochastic Differential Equations,” *The Journal of Mathematical Neuroscience* **5**, 8 (2015).

- [16] Markus F Weber and Erwin Frey, “Master equations and the theory of stochastic path integrals,” *Reports on Progress in Physics* **80**, 046601 (2017).
- [17] Leticia F Cugliandolo and Vivien Lecomte, “Rules of calculus in the path integral representation of white noise Langevin equations: the Onsager–Machlup approach,” *Journal of Physics A: Mathematical and Theoretical* **50**, 345001 (2017).
- [18] Leticia F Cugliandolo, Vivien Lecomte, and Frédéric van Wijland, “Building a path-integral calculus: a covariant discretization approach,” *Journal of Physics A: Mathematical and Theoretical* **52**, 50LT01 (2019).
- [19] Thibaut Arnoux De Pirey, Leticia F. Cugliandolo, Vivien Lecomte, and Frédéric Van Wijland, “Path integrals and stochastic calculus,” *Advances in Physics* **71**, 1–85 (2023).
- [20] D. Dacunha-Castelle and D. Florens-Zmirou, “Estimation of the coefficients of a diffusion from discrete observations,” *Stochastics* **19**, 263–284 (1986).
- [21] W.R. Gilks, S. Richardson, and David Spiegelhalter, eds., *Markov Chain Monte Carlo in Practice*, 0th ed. (Chapman and Hall/CRC, 1995).
- [22] Ola Elerian, “A note on the existence of a closed form conditional transition density for the Milstein scheme,” (1998).
- [23] Y K Tse, Xibin Zhang, and Jun Yu, “Estimation of hyperbolic diffusion using the Markov chain Monte Carlo method,” *Quantitative Finance* **4**, 158–169 (2004).
- [24] Alexandros Beskos, Gareth Roberts, Andrew Stuart, and Jochen Voss, “MCMC METHODS FOR DIFFUSION BRIDGES,” *Stochastics and Dynamics* **08**, 319–350 (2008).
- [25] Ming Lin, Rong Chen, and Per Mykland, “On Generating Monte Carlo Samples of Continuous Diffusion Bridges,” *Journal of the American Statistical Association* **105**, 820–838 (2010).
- [26] Alain Durmus, Gareth O. Roberts, Gilles Vilmart, and Konstantinos C. Zygalakis, “Fast Langevin based algorithm for MCMC in high dimensions,” arXiv:1507.02166 [math] (2016), arXiv: 1507.02166.
- [27] Sudipta Bera, Shuvojit Paul, Rajesh Singh, Dipanjan Ghosh, Avijit Kundu, Ayan Banerjee, and R. Adhikari, “Fast Bayesian inference of optical trap stiffness and particle diffusion,” *Scientific Reports* **7**, 41638 (2017).
- [28] Susanne Pieschner and Christiane Fuchs, “Bayesian inference for diffusion processes: using higher-order approximations for transition densities,” *Royal Society Open Science* **7**, 200270 (2020).
- [29] Hiroshi Fujisaki, Motoyuki Shiga, and Akinori Kidera, “Onsager–Machlup action-based path sampling and its combination with replica exchange for diffusive and multiple pathways,” *The Journal of Chemical Physics* **132**, 134101 (2010).
- [30] Hiroshi Fujisaki, Motoyuki Shiga, Kei Moritsugu, and Akinori Kidera, “Multiscale enhanced path sampling based on the Onsager–Machlup action: Application to a model polymer,” *The Journal of Chemical Physics* **139**, 054117 (2013).
- [31] M I Dykman and M A Krivoglaz, “Theory of fluctuational transitions between stable states of a nonlinear oscillator,” *Journal of Experimental and Theoretical Physics* , 8 (1979).
- [32] M. I. Dykman, P. V. E. McClintock, V. N. Smelyanski, N. D. Stein, and N. G. Stocks, “Optimal paths and the prehistory problem for large fluctuations in noise-driven systems,” *Physical Review Letters* **68**, 2718–2721 (1992).
- [33] Christian Maes and Karel Netočný, “Time-Reversal and Entropy,” *Journal of Statistical Physics* **110**, 269–310 (2003).
- [34] Udo Seifert, “Entropy production along a stochastic trajectory and an integral fluctuation theorem,” *Physical Review Letters* **95**, 040602 (2005), arXiv: cond-mat/0503686.
- [35] Michael E. Cates, Étienne Fodor, Tomer Markovich, Cesare Nardini, and Elsen Tjhung, “Stochastic Hydrodynamics of Complex Fluids: Discretisation and Entropy Production,” *Entropy* **24**, 254 (2022).
- [36] Miguel V. Moreno, Daniel G. Barci, and Zochil González Arenas, “Conditional probabilities in multiplicative noise processes,” *Physical Review E* **99**, 032125 (2019).
- [37] Alexander N. Drozdov, “Exponential power series expansion for the propagator of general diffusion processes,” *Physica A: Statistical Mechanics and its Applications* **196**, 283–312 (1993).
- [38] Alexander N. Drozdov, “An accurate power series expansion for path integrals on curved manifolds,” *Zeitschrift für Physik B Condensed Matter* **90**, 241–245 (1993).
- [39] Alexander N. Drozdov, “High-accuracy discrete path integral solutions for stochastic processes with noninvertible diffusion matrices,” *Physical Review E* **55**, 2496–2508 (1997).
- [40] Alexander N. Drozdov, “High-accuracy discrete path integral solutions for stochastic processes with noninvertible diffusion matrices. II. Numerical evaluation,” *The Journal of Chemical Physics* **107**, 3505–3520 (1997).
- [41] Yacine Aït-Sahalia, “Maximum Likelihood Estimation of Discretely Sampled Diffusions: A Closed-form Approximation Approach,” *Econometrica* **70**, 223–262 (2002).
- [42] Yacine Aït-Sahalia, “Closed-form likelihood expansions for multivariate diffusions,” *The Annals of Statistics* **36** (2008), 10.1214/009053607000000622.
- [43] Benjamin Sorokin, Gil Ariel, and Tomer Markovich, “Consistent expansion of the Langevin propagator with application to entropy production,” (2024), arXiv:2405.13855 [cond-mat].
- [44] Peter E. Kloeden and Eckhard Platen, *Numerical Solution of Stochastic Differential Equations* (Springer Berlin Heidelberg, Berlin, Heidelberg, 1992).
- [45] Julian Kappler, “Python module for (symbolic) evaluation of the short-time fokker-planck propagator to arbitrary accuracy, <https://github.com/juliankappler/pystfp>,” .
- [46] Aaron Meurer, Christopher P. Smith, Mateusz Paprocki, Ondřej Čertík, Sergey B. Kirpichev, Matthew Rocklin, AMiT Kumar, Sergiu Ivanov, Jason K. Moore, Sartaj Singh, Thilina Rathnayake, Sean Vig, Brian E. Granger, Richard P. Muller, Francesco Bonazzi, Harsh Gupta, Shivam Vats, Fredrik Johansson, Fabian Pedregosa, Matthew J. Curry, Andy R. Terrel, Štěpán Roučka, Ashutosh Saboo, Isuru Fernando, Sumith Kulal, Robert Cimrman, and Anthony Scopatz, “SymPy: symbolic computing in python,” *PeerJ Computer Science* **3**, e103 (2017).
- [47] L. Onsager and S. Machlup, “Fluctuations and Irreversible Processes,” *Physical Review* **91**, 1505–1512 (1953).
- [48] Peter Arnold, “Symmetric path integrals for stochastic equations with multiplicative noise,” *Physical Review E*

- 61**, 6099–6102 (2000).
- [49] Sadri Hassani, *Mathematical methods: for students of physics and related fields*, 2nd ed. (Springer, New York, NY, 2009).
- [50] Julian Kappler and Ronojoy Adhikari, “Stochastic action for tubes: Connecting path probabilities to measurement,” *Physical Review Research* **2** (2020), 10.1103/PhysRevResearch.2.023407.
- [51] Julian Kappler and Ronojoy Adhikari, “Sojourn probabilities in tubes and pathwise irreversibility for It^o processes,” arXiv:2009.04250 [cond-mat, physics:physics] (2020), arXiv: 2009.04250.
- [52] R. F. Pawula, “Approximation of the Linear Boltzmann Equation by the Fokker-Planck Equation,” *Physical Review* **162**, 186–188 (1967).
- [53] R. Friedrich, Ch. Renner, M. Siefert, and J. Peinke, “Comment on “Indispensable Finite Time Corrections for Fokker-Planck Equations from Time Series Data”,” *Physical Review Letters* **89**, 149401 (2002).
- [54] Julia Gottschall and Joachim Peinke, “On the definition and handling of different drift and diffusion estimates,” *New Journal of Physics* **10**, 083034 (2008).
- [55] Leonardo Rydin Gorjão, Dirk Witthaut, Klaus Lehnertz, and Pedro G. Lind, “Arbitrary-Order Finite-Time Corrections for the Kramers–Moyal Operator,” *Entropy* **23**, 517 (2021).
- [56] Udo Seifert, “From Stochastic Thermodynamics to Thermodynamic Inference,” *Annual Review of Condensed Matter Physics* **10**, 171–192 (2019).
- [57] Ken Sekimoto, *Stochastic energetics*, Lecture notes in physics No. 799 (Springer, Heidelberg ; New York, 2010) oCLC: ocn462919832.
- [58] Detlef Dürr and Alexander Bach, “The Onsager-Machlup function as Lagrangian for the most probable path of a diffusion process,” *Communications in Mathematical Physics* **60**, 153–170 (1978).
- [59] Julian Kappler and Ronojoy Adhikari, “Measurement of irreversibility and entropy production via the tubular ensemble,” *Physical Review E* **105**, 044107 (2022).
- [60] Stefano Bo, Soon Hoe Lim, and Ralf Eichhorn, “Functionals in stochastic thermodynamics: how to interpret stochastic integrals,” *Journal of Statistical Mechanics: Theory and Experiment* **2019**, 084005 (2019).
- [61] Julian Kappler and Ronojoy Adhikari, “Irreversibility and entropy production along paths as a difference of tubular exit rates,” arXiv:2007.11639 [cond-mat, physics:physics] (2020), arXiv: 2007.11639.
- [62] Pauli Virtanen, Ralf Gommers, Travis E. Oliphant, Matt Haberland, Tyler Reddy, David Cournapeau, Evgeni Burovski, Pearu Peterson, Warren Weckesser, Jonathan Bright, Stéfan J. van der Walt, Matthew Brett, Joshua Wilson, K. Jarrod Millman, Nikolay Mayorov, Andrew R. J. Nelson, Eric Jones, Robert Kern, Eric Larson, C J Carey, İlhan Polat, Yu Feng, Eric W. Moore, Jake VanderPlas, Denis Laxalde, Josef Perktold, Robert Cimrman, Ian Henriksen, E. A. Quintero, Charles R. Harris, Anne M. Archibald, Antônio H. Ribeiro, Fabian Pedregosa, Paul van Mulbregt, and SciPy 1.0 Contributors, “SciPy 1.0: Fundamental Algorithms for Scientific Computing in Python,” *Nature Methods* **17**, 261–272 (2020).